Hindawi
Advances in Civil Engineering
Volume 2019, Article ID 6975751, 31 pages
https://doi.org/10.1155/2019/6975751

Review Article

Crack Initiation, Propagation, and Failure Characteristics of Jointed Rock or Rock-Like Specimens: A Review

Ri-hong Cao,[1,2,3] Ping Cao,[1] Hang Lin,[1] Xiang Fan,[3,4] Chunyang Zhang,[5] and Taoying Liu[1,4]

[1]*School of Resources and Safety Engineering, Central South University, Changsha, Hunan 410083, China*
[2]*School of Civil, Environmental and Mining Engineering, The University of Western Australia, Perth 6009, Australia*
[3]*Engineering laboratory of Spatial Information Technology of Highway Geological Disaster Early Warning in Hunan Province, Changsha University of Science & Technology, Changsha 410114, Hunan, China*
[4]*School of Highway, Chang'an University, Xi'an 710064, China*
[5]*School of Resources and Environment Engineering, Wuhan University of Technology, Wuhan 430070, China*

Correspondence should be addressed to Hang Lin; linhangabc@126.com

Received 15 March 2018; Accepted 13 December 2018; Published 17 February 2019

Academic Editor: Flavio Stochino

Copyright © 2019 Ri-hong Cao et al. This is an open access article distributed under the Creative Commons Attribution License, which permits unrestricted use, distribution, and reproduction in any medium, provided the original work is properly cited.

Rock masses are heterogeneous materials containing a large number of discontinuities, and the failure of the natural rock mass is induced by the crack propagation and coalescence of discontinuities, especially for the rock mass around tunnel or underground space. Because the deformation or failure process of jointed rock mass exhibits strongly nonlinear characteristics, it is also very difficult to predict the strength and failure modes of the rock mass. Therefore, it is very necessary to study the failure mechanisms of jointed rock mass under different stress conditions. Apart from the stress condition, the discontinuities geometry also has a significant influence on the mechanical behavior of jointed rock mass. Then, substantial, experimental, and numerical efforts have been devoted to the study of crack initiation, propagation, and coalescence of rock or rock-like specimens containing different kinds of joints or fissures. The purpose of this review is to discuss the development and the contribution of the experiment test and numerical simulation in failure behavior of jointed rock or rock-like specimens. Overall, this review can be classified into three parts. It begins by briefly explaining the significance of studying these topics. Afterwards, the experimental and numerical studies on the strength, deformation, and failure characteristics of jointed rock or rock-like materials are carried out and discussed.

1. Introduction

After hundred millions years of geological movements, there is a large number of discontinuities in natural rock mass. The natural rock mass is clearly a kind of heterogeneity material [1], and the discontinuities have a great influence on the mechanical behavior of rock mass. In most engineering cases, such as roadway excavation, rock slope, and pillars in deep mining activities, there often requires the estimation of the strength and failure characteristics of a rock mass that contains a large number of discontinuities [2–5]. And, many engineering disasters are closely associated with crack initiation and propagation between preexisting joints (Figure 1). For example, the collapse of the Malpasset arch dam (French) results from the crack propagation in rocks of bam foundation. And, there are also many excavation activities that have to face with the crack propagation and coalescence in rock mass. Then, it is very necessary to investigate the strength and failure characteristics of jointed rock mass. At the same time, the crack initiation, propagation, and failure characteristics are of great interest to engineers and scientists.

This review concentrates on experimental techniques for mechanical behavior of jointed natural rocks or brittle rock-like materials. All literature available to the authors (in total, 196 references) concerning this topic was extensively reviewed. This review is structured in the following way. After "Introduction," the synthesis, analysis, and evaluation

(a) (b)

Figure 1: Discontinuities in rock engineering. (a) Joints in rock slope. (b) Joints in pillars [6].

are discussed in Section 2. In Section 3, the loading techniques are discussed, and for each loading pattern, the mechanical characteristics of the specimen with different joint geometry parameters have also been discussed. Section 4 presents widely used numerical simulation techniques for crack initiation, propagation, and failure process of rock or rock-like materials. Finally, a brief summary and some prospective research are presented.

2. Experimental Materials and Specimen Preparation

In recent years, the failure behavior of jointed rock mass has been widely studied by scholars, and the experimental test is the most common way. So far, many types of materials have been employed for such tests. As we all know, the ideal material for experiment is the natural rocks. And, there are many kinds of rocks which have been used in previous studies, such as granite, sand stone, and marble (Table 1). As shown in Figure 2, the specimens are made from natural rocks. The fissures in the specimen are open, and the fissure is produced via high-pressure water-jet cutting method.

Apart from the natural rocks, many kinds of rock-like materials have also been widely used by scholars, such as glass [7], Columbia Resin 39 [8], and molded gypsum [9–16]; the most common among them is gypsum and cement mortar (Table 1). The cement mortar is used because the main framework of the specimen consists of sand and cement, and the sand can provide frictional behavior of the modelling material. Then, the cement mortar is suitable for modelling rock mass. Compared to the cement mortar, the frictional behavior on the failure plane is inapparent.

For most rock-like material specimens, the fissure or joint was mainly handcrafted. In Figures 3(a)–3(c), the open fissure in PMMA, gypsum, and cement mortar specimen are shown, respectively. In the specimen preparation, preexisting fissures are created by inserting metal sheets into the fresh mixture at the desired locations of the fissures and removing them after rock-like materials become hardened.

At the same time, in the previous studies, the closed fissure or joint can also be created by scholars through different ways. In Figure 4(a), the ubiquitous joints created by inserting mica sheets into fresh cement mortar are shown [20]. The mica sheet has also been used by other scholars to investigate the failure characteristics of jointed rock mass [21]. Because of the strength of the mica sheet and relatively low interface between mica sheet and mortar, the mica sheet is suitable for modelling the joints which can be filled up with clay. In Figure 4(b), the closed fissure created by inserting steel sheets into the mortar is shown [22]. During preparation process, the steel sheets were removed carefully after about 3 ± 5 min of curing, and then, further expansion of the plaster mixture during curing closed the slots, thereby creating preexisting cracks with closed surfaces. And, to obtain a crack surface with different roughness, three kinds of roughness of the stainless steel sheets were used. Like the fissure shown in Figure 4(c), the plat closed fissure is created by inserting a video tape strip [23]. The video tape strips are pulled out of the mold 30 min after vibration, and the gypsum is soft enough and can expand to fill the gap left behind by the strips. Moreover, instead of pull out, some scholars also attempt to create closed joint via the left behind the galvanized sheets in the mixture [24]. Actually, the stiff of galvanized sheet is far below the rock-like material. Because the interface is relatively smooth, the slide effect on the interface is also obvious; it is similar to the mica sheet-mortar interface.

3. Failure Characteristics of Jointed Rocks or Rock-Like Materials under Different Loading Methods

3.1. Uniaxial Compressive Loading. The uniaxial compressive loading is the most common load mode in previous works. And, in many engineering cases, the rock mass failure occurs from the crack coalescence under axial loading. In Figure 5, the pillar failure from the coalescence between two inclined fissures is shown. It is clear that the preexisting fissure has a great influence on the strength, deformation, and failure characteristics of rock mass. In order to better understand the failure process of engineering rock masses, experimental studies have focused on the jointed specimens that contain preexisting joints.

Table 1: Major materials for the specimen in testing the failure behavior of jointed rocks.

Specimen material		Fissure type	References
Natural rocks	Granite	Open	Lee and Jeon [17]; Morgan et al. [25]; Yin et al. [26]; Yin et al. [27]; Yang [18, 28–31]; Petit and Barquins [32]; Lu et al. [33]; Wang et al. [34]; Wei [35–37]; Fan [38]
	Sandstone	Open	
		Closed	Da Huang et al. [39];
	Marble	Open	Li et al. [40]; Brooks et al. [41]; Yang et al. [42]; Wong and Einstein [15, 16, 43]; Cheng et al. [44]; Chen et al. [45]; Wong RHC et al. [46]; Ferrero et al. [47]; Xeidakis et al. [48]; Migliazza et al. [49]
	Diastone	Open	Lee and Jeon [17]
	Opalinus shale	Open	Morgan and Einstein [50]
	Limestone	Open	Ingraffea and Heuze [51]
Cement mortar		Open	Prudencio and Jan [52]; Cao et al. [19]; Cao et al. [53, 54]; Liu [55]; Feng [56, 57]; Zhao et al. [58]; Jin et al. [59]; Omer [60, 61]; Hadi Haeri et al. [62]; Liu [63]; Huang et al. [64]; Jin [65]; Liu et al. [66]; Sarfarazi et al. [67]; Ghazvinian et al. [68]; Zhang et al. [69]
		Closed	Wasantha et al. [70]; Cao et al. [20, 71–74]; Zhang et al. [21]; Lin [75, 76]
Gypsum		Open	Bobet [77]; Bobet and Einstein [11]; Park and Bobet [23]; Sagong and Bobet [14, 78]; Shen [10]; Liu et al. [79]; Yang et al. [80]; Cheng et al. [81]; Zhou et al. [82]; Wong and Einstein [15, 16, 43]; Reyes and Einstein [13]; Gehle and Kutter [83]; Eleni and Theodoros [84]
		Closed	Park and Bobet [23, 85]; Shen [10]; Wong and Chou [22]; Kulatilake et al. [24]; Wong et al. [86]; Einstein and Jeng [87]; Chen et al. [88]
PMMA		Open	Lee and Jeon [17]; Huang and Wong [89, 90]; Canon [91]
Resin		Open	Dyskin et al. [92]; Sahouryeh et al. [93]; Guo et al. [94]
		Closed	Tang et al. [95]; Ju et al. [96]; Dyskin [92, 97]; Fu et al. [98]
Glass		Open	Bieniawski [99]; Hoek and Bieniawski [7]; Brace and Bombolakis [100];

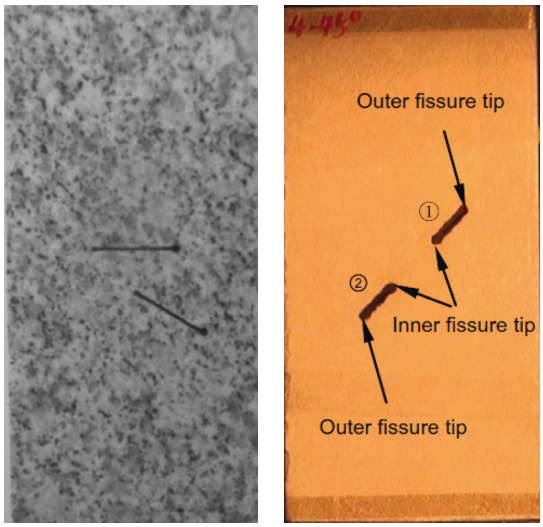

(a) (b)

Figure 2: Jointed specimens are made of natural rocks. (a) Hwangdeung granite [17]. (b) Sand stone [18].

For the specimen with single joint or fissure, under uniaxial loading, two types of cracks will initiate from the preexisting fissure, namely, wing and secondary cracks [7, 28, 40, 92, 101, 102]. With further loading, new cracks propagate and reach the edge of the specimen and result in overall failure. In Figure 6, the various crack types initiated from the preexisting flaws identified by Yang et al. [28] and Wong and Einstein [43] are shown. Furthermore, substantial experimental efforts have illustrated cracks with similar characteristics in the specimens with single fissure [10, 11, 34, 77, 78, 99, 103–105].

Apart from the single joint, the coalescence pattern between cracks has been investigated via experiment tests as well. For a specimen containing two or three fractures, some studies focused on crack coalescence between parallel fractures [12, 14, 18, 22, 23, 40, 82, 101, 106–112]. In Figures 7(b) and 7(c), the experimental results from Wong and Einstein [15] and Sagong and Bobet [14] are shown, respectively. Wong and Chau [22] presented nine types of coalescence pattern between two parallel fissures (Figure 7(c)). Overall, the coalescence pattern mainly concentrates on tensile pattern, shear pattern, and mixed pattern. For the tensile or shear pattern, the coalescence results from the tensile or shear crack propagation and linkage. However, for the mixed pattern, it is the combination of tensile and shear crack. At the same time, there are many kinds of combinations.

For the unparallel fissures, Lee and Jeon [17] investigated the penetration mode between two unparallel fissures by using PMMA, Hwangdeung granite, and Diastone. The unparallel fissures were created through the water-jet system. The unparallel fissure is the combination of a horizontal fissure and an inclined fissure underneath, and the inclined fissure had an inclination angle of 30°–90° in 15° intervals. Under uniaxial compressive loading, coalescence occurred mainly through the tensile cracks or tensile and shear cracks (Figure 8). In addition, the crack initiation and coalescence stresses were analysed. The results indicated that the shielding effect of the horizontal fissure plays an important role in the stresses, and the stresses reached a critical point when the inclination angle is 60°.

Except for the literatures mentioned above, there are also laboratory tests conducted by other scholars to investigate the failure behavior of the specimen with unparallel fissures. Zhang et al. [69] studied crack

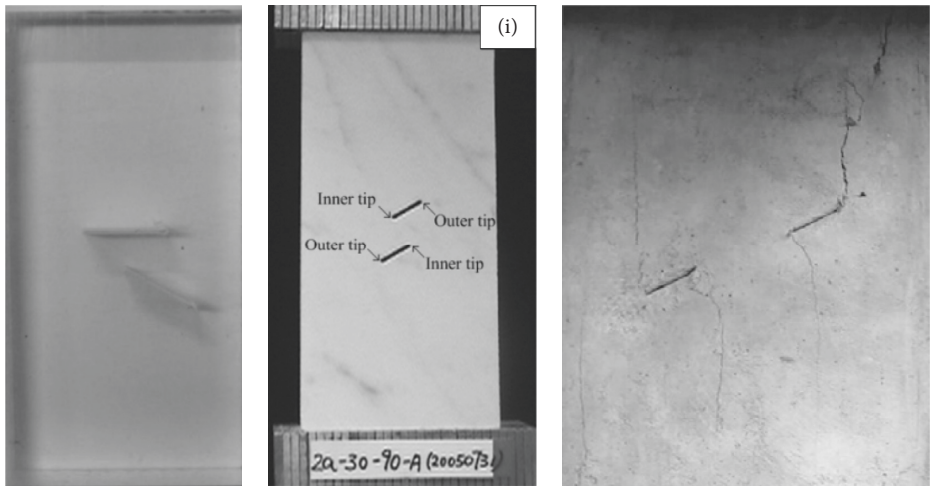

(a) (b) (c)

Figure 3: Open fissures in rock-like material specimens. (a) PMMA [17]. (b) Gypsum [15]. (c) Cement mortar [19].

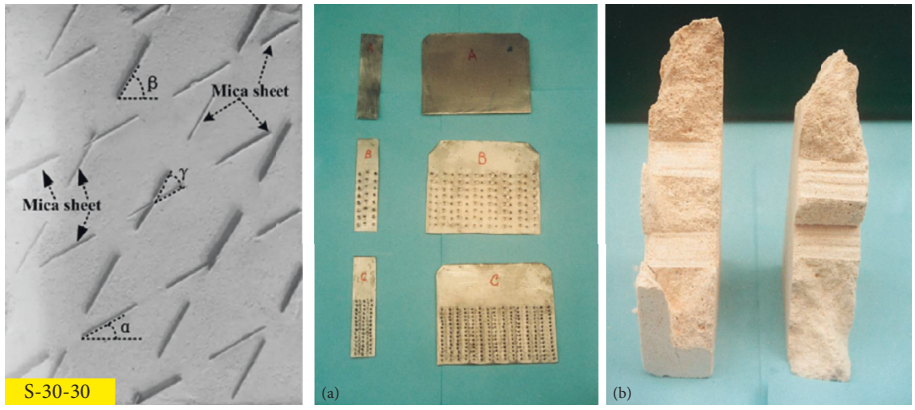

(a) (b)

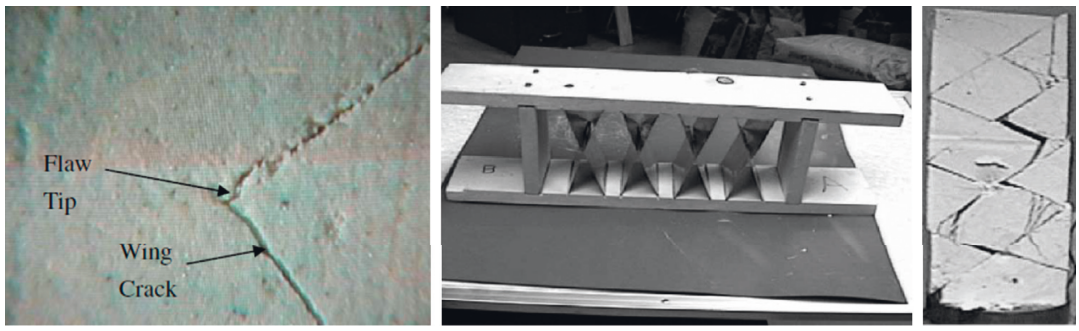

(c) (d)

Figure 4: Closed fissures created by different kinds of methods. (a) Mica sheet [20]. (b) Steel sheets [22]. (c) Video tape strip [23]. (d) Galvanized sheets [24].

coalescence between two nonparallel flaws; five types of linkage were observed between two flaws: tensile crack linkage, tensile crack linkage with shear coalescence at the tip, shear crack linkage, mixed linkage, and indirect crack linkage. Using photographic monitoring and acoustic emissions monitoring techniques, Yang et al. [113] investigated the relationship between the real-time crack coalescence process and axial stress-time behavior for red sandstone containing two unparallel fissures.

In addition to studies on parallel or unparallel fractures, the mechanical behavior of multifissure specimens under uniaxial loading are also well discussed in the literature. As mentioned above, two types of cracks initiated from the tips of fissure. With further loading, new cracks propagate and link with others to form overall failure. In the previous studies, many kinds of joint geometry are also considered, such as joint inclination angel [53, 71, 80, 88], joint distance [53, 71, 80, 88], and overlap distance [88]. Cao et al. [53]

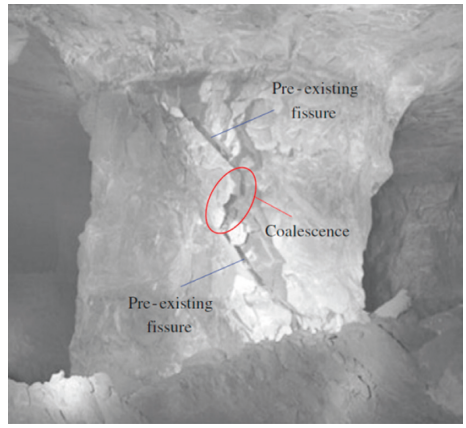

Figure 5: Coalescence along two angular discontinuities in pillar fissure [6].

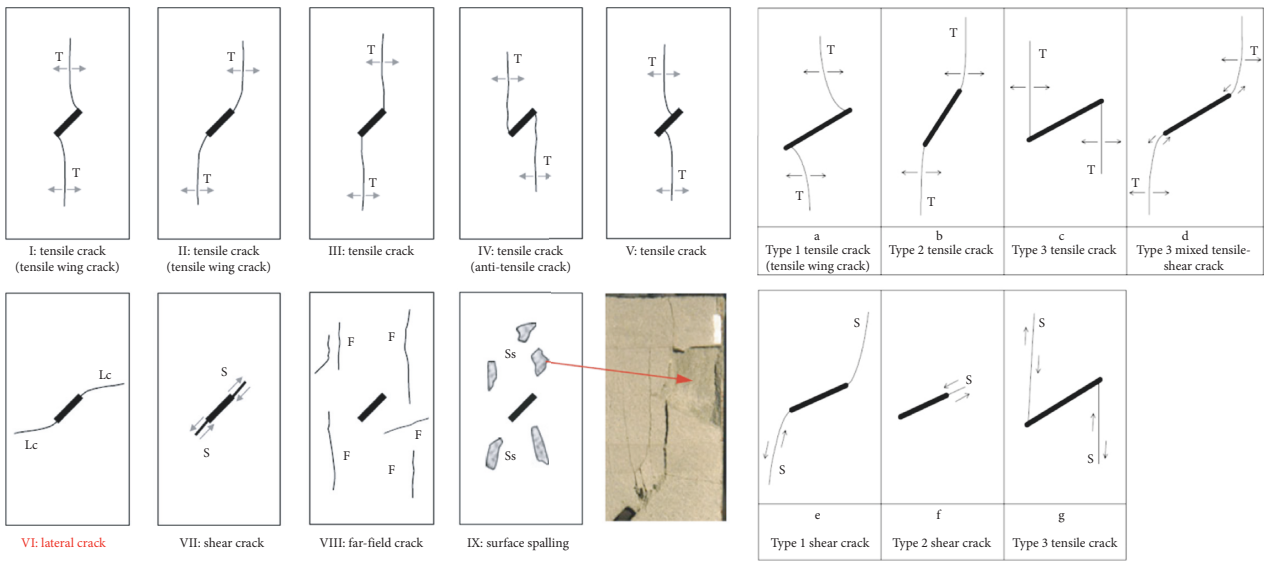

Figure 6: Various crack types initiated from the preexisting flaws identified by scholars. (a) Yang, 2011 [18]. (b) Wong, 2009 [43].

conducted laboratory tests on physical models of rock with nonpersistent joints. The specimen is made of cement mortar, and the dimensions (height × width × thickness) are 200 × 150 × 30 mm. The preexisting fissures in the specimens are created by inserting metal shims into the fresh mortar and removing it after it becomes hardened. There are four kinds of inclination angles in the specimen: 25°, 45°, 75°, and 90°. And, for each angle, the fissure number varied from 5 to 20 at 5-unit increments. The experimental test results indicated that the strength of the specimen increases with the increasing of the joint inclination angle and decreases with the increasing of the fissure number. Moreover, the failure modes of specimens can be classified into four categories: mixed failure, stepped path failure, Shearing failure, and intact failure (Figure 9).

For the specimen with different inclination, Yang's [88] result indicates that the jointed rock mass is in significant dependence of the joint orientation, and four kinds of failure modes are identified: tensile failure across the joint plane, shear failure along the joint plane, tensile failure along the joint plane, and intact material failure. For the ubiquitous joint, Cao et al. [20] identified four types of failure pattern through experimentation on rock-like specimens, the failure patterns of the multiple jointed specimen including stepped path failure, planar failure, shear-I failure, and shear-II failure (Figure 10).

3.2. Biaxial and Triaxial Loading. As mentioned above, the failure process of jointed rocks or rock-like materials has been fully investigated by scholars. However, the confining pressure also has a great influence on the mechanical behavior of jointed rock mass. For the failure behavior considering a confining pressure, experimental studies have been conducted via biaxial or triaxial loading. Bobet and Einstein [11] investigated the fracture coalescence in the gypsum specimen with two open or closed preexisting fissures under biaxial compression. The tests showed wing cracks appeared under unconfined and slightly confined compressive loads and disappeared entirely at high confining stresses. Mughieda and

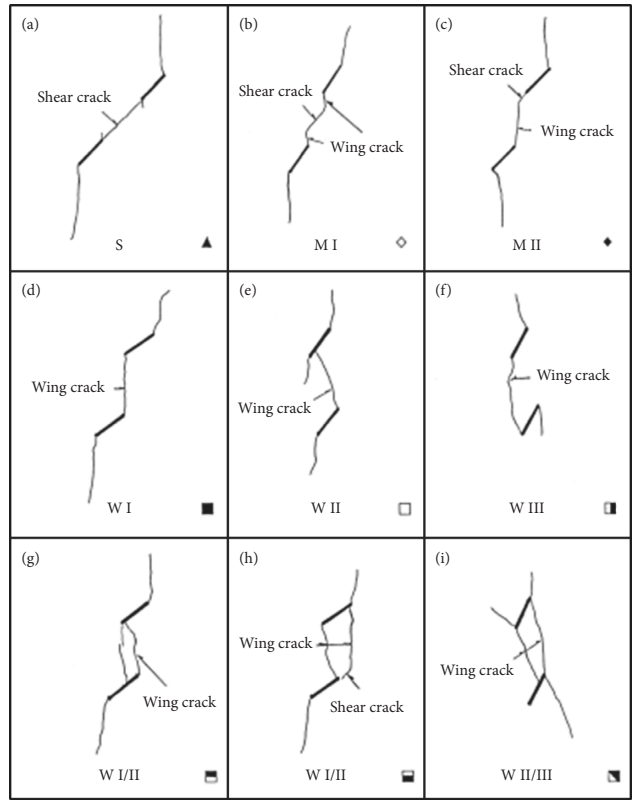

(a)

Category	Coalescence patterens	Crack types involved
1		No coalescence
2	(2 cracks) (3 cracks)	Indirect coalescene by two or multiple cracks (crack types vary)
3		Type 2 S crack(s)
4		Type 1 S crack(s)
5		One or more type 2 S crack(s) and type 2 T crack segments between inner flaw tips
6		Type 2 T crack(s). There may be occasional short S segment present along the coalescence crack
7		Type 1 T crack(s)
8		Flaw tips at the same inside linked by T crack(s) not displaying wing appearance (crack type not classified). There may be occasional short S segments present along the coalescence crack
9		Type 3 T crack(s) linking right tip of the top flaw and left tip of the bottom flaw. There may be occasional short S segments present along the coalescence crack

(b)

Figure 7: Continued.

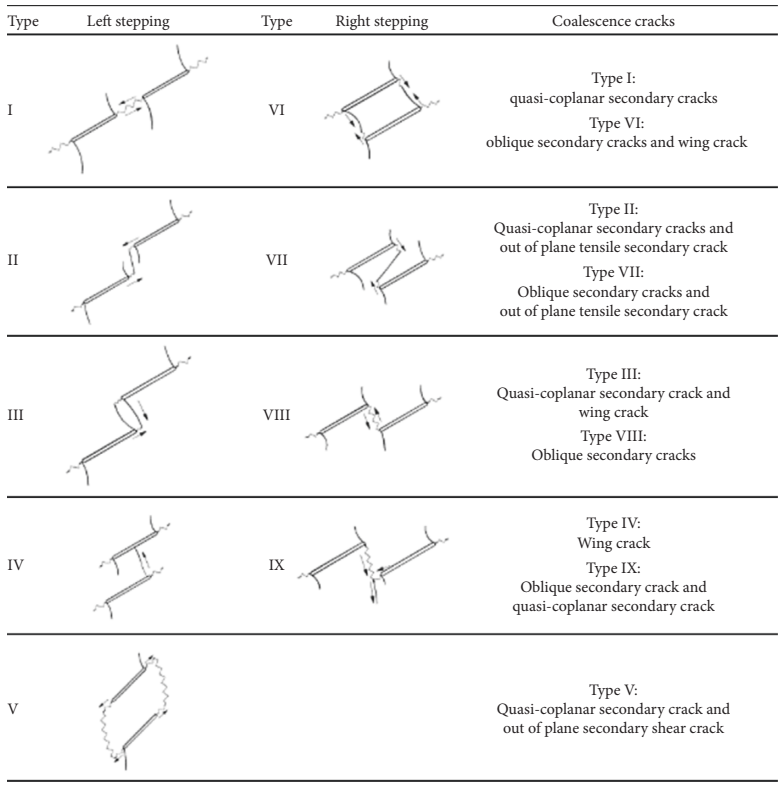

(c)

Figure 7: Classification of the coalescence types in the previous studies. (a) Wong and Chau [22]. (b) Wong and Einstein [15]. (c) Sagong and Bobet [14].

Karasneh [61] investigated the coalescence mode between cracks through a series of biaxial compression tests on rock-like specimens. The dimensions (height × width × thickness) of each specimen are 63.5 × 27.9 × 20.3 cm (Figure 11). The geometry parameters of preexisting joints include joint inclination angle α and bridge inclination angle β; three kinds of lateral stress were used: 0.35 MPa, 0.7 MPa, and 1.5 MPa on each specimen. Under biaxial loading, three types of coalescence modes were observed between preexisting joints: tensile, shear, and tensile + shear coalescence.

Prudencio and Jan [52] carried out biaxial experiments on rock-like specimens containing multifissures; the dimensions (height × width × thickness) of each specimen are 300 × 150 × 50 mm. Four kinds of joint geometry parameters were considered: persistence (k), spacing (L_r/d), dip angle (β), and angle of overlap (γ). The experimental results showed three basic failure modes: failure through a planar surface, stepped failure, and failure by the rotation of new blocks (Figure 12). Furthermore, the strength and deformation of the jointed specimen are related to the failure mode. To be specific, the specimen with planar failure and stepped failure exhibits higher strength and small failure strain. However, the rotational failure mode is associated with low strength and large deformation.

For the triaxial compression, there are mainly two types of loading methods, through either a pressure or displacement boundary condition [114]. As shown in Figure 13, for the conventional triaxial test, the specimen is cylindrical and has been put inside a pressure chamber and isotropically loaded by hydrostatic pressure using various confining fluids (e.g., air, water, and hydraulic oil).

Huang et al. [39] conducted conventional triaxial compression experiments on sandstone specimens with two closed nonoverlapping fissures. As shown in Figure 14, four types of sandstone specimens were tested. Moreover, in order to form closed fissures, the mixture of water, cement, and sand has been used to fill up the open fissures. The test results show that the arrangement of the fissure has a significant influence on the deformation, strength, and failure pattern of the specimen. Compared with the stress-strain curves of the intact specimen (Type A in Figure 14), the post-peak curves obtain from the precracked rock specimens exhibit obvious fluctuation, especially for Type D in Figure 14. For the Type B, the stress-strain curves exhibit Z-shape characteristics and show a double-peak stress. Moreover, the influence of fissure geometry is greater than that of confining pressure. In addition, the stress for crack initiation, dilation, and the peak strength of jointed sandstone specimens is significantly lower than that of intact rock.

Using a combination of experiments and PFC (3D), Hang et al. [115] investigated the internal damage behavior of rock under conventional triaxial compression tests. As shown in Figure 15, there are two unparallel fissures in the cylindrical specimens (50 mm diameter and 100 mm height). And, four kinds of confining pressures have been considered: 0 MPa, 5 MPa, 15 MPa, and 25 MPa. The results show that the crack

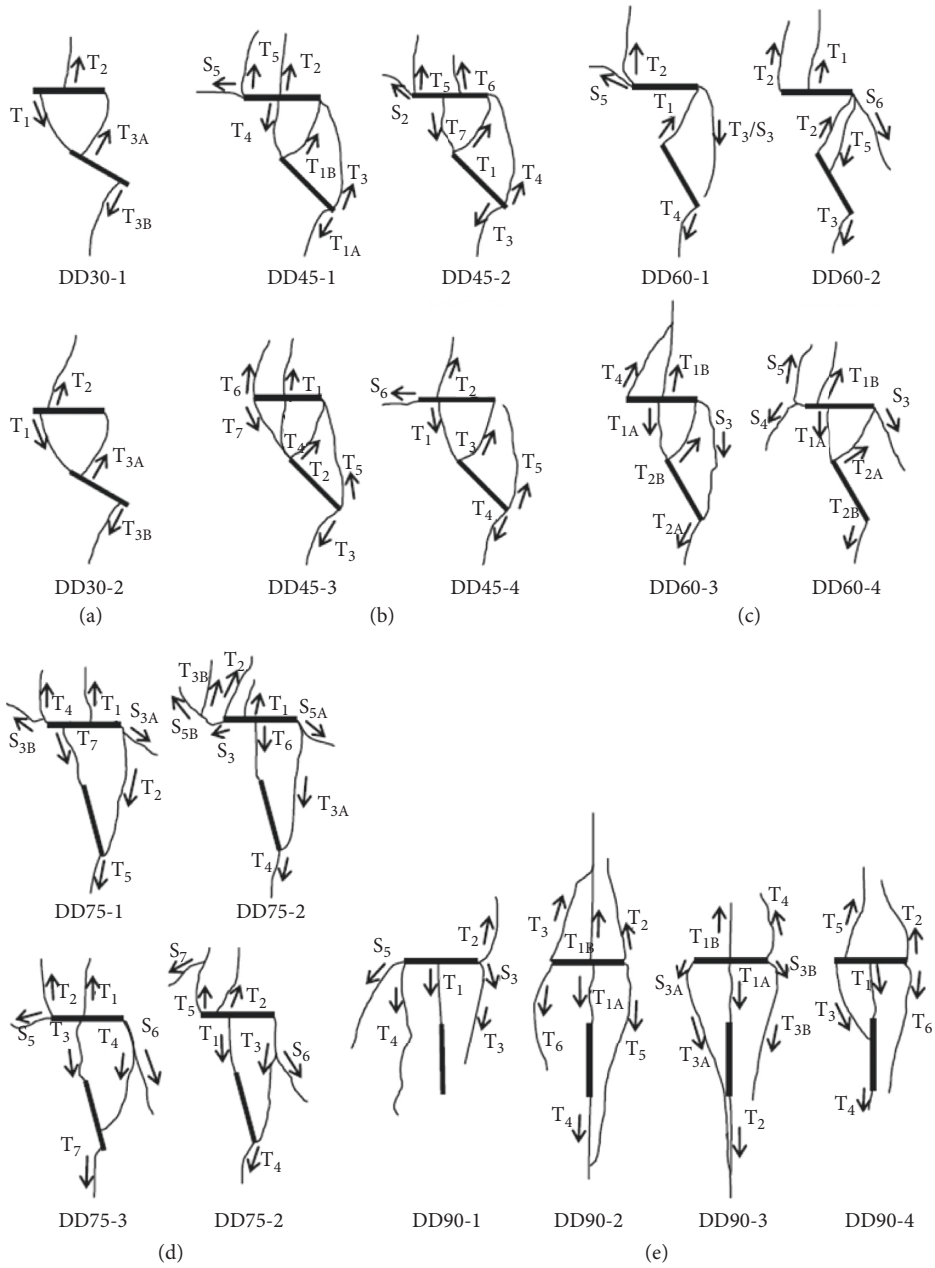

Figure 8: Sketch of the observed cracks around the bridge area in the Diastone specimens [17].

evolution and failure characteristics are dependent on the fissure geometry and confining pressure. At the same time, when the confining pressure is low, the failure mode of the specimen is mainly affected by fissure geometry. When the confining pressure is high, the effect of confining pressure on the failure mode is greater than that of fissure geometry.

However, for the true triaxial compression, there are few studies focused on the specimen with fissure or joint. Most of the literatures concentrated on the mechanical behavior of intact rocks under true triaxial compression. Chen and Feng [116] carried out true triaxial unloading tests on new granite specimens, and the rock triaxial strength has also been discussed. With unloading, the minor principal stress, Du et al. [117] investigated true triaxial strength and failure modes of cubic rock specimens (Figure 16). The triaxial tests have been carried on granite, sandstone, and cement mortar cubic specimens. Under true triaxial unloading condition, the test results show that both the strength and failure modes of cubic rock specimens are affected by the intermediate principal stress. The end effect of specimen seems not to play an important role in strength and failure modes of cubic specimen under triaxial tests. For the hard rock, when σ_2 increases to a critical value, the fracture angle of the specimen may change from shear to slabbing failure. However, for medium strong and weak rocks, they exhibit shear failure with a large amount of plastic deformation.

3.3. Tension Loading. For the tension loading, there are two types of standard methods: direct tension [118, 119] and

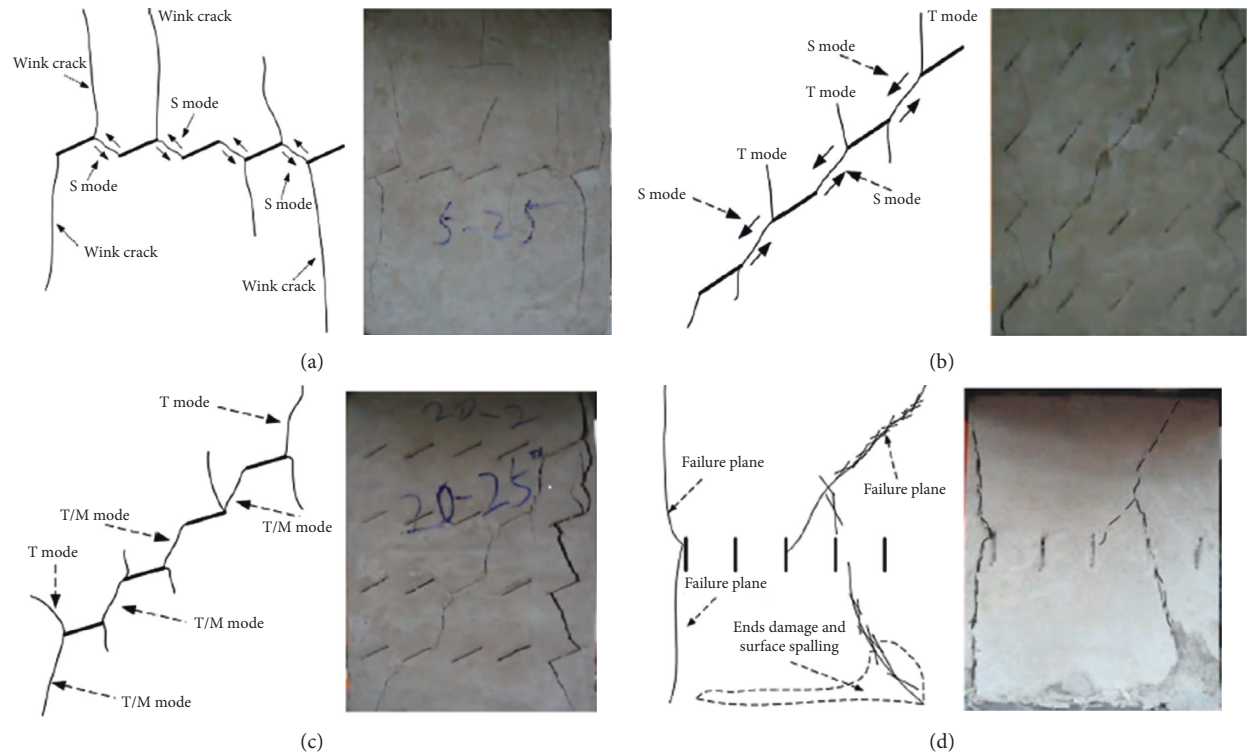

FIGURE 9: Crack coalescence in different failure modes [53]. (a) Mixed failure. (b) Shearing failure. (c) Stepped path failure. (d) Intact failure.

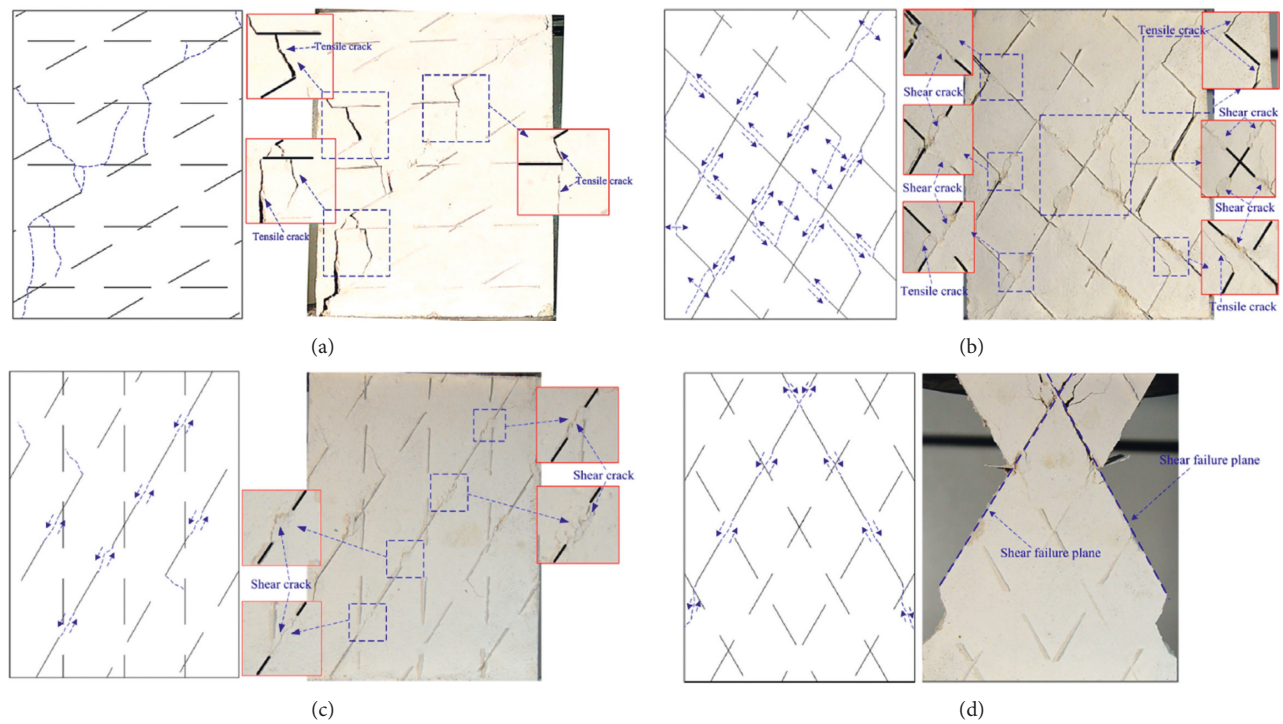

FIGURE 10: Crack coalescence in different failure modes [20]. (a) Stepped path failure. (b) Planar failure. (c) Shear-I failure. (d) Shear-II failure.

indirect tension [119, 120] tests. And, these two kinds of methods were suggested by the ISRM and ASTM for determining the quasistatic tensile strength of rock materials. For the crack initiation under tension loading, the Brazilian tensile test is the most common in previous works. Khanlari et al. [121] conducted Brazilian tensile tests on laminated sandstone to investigate the tensile strength and failure pattern of jointed rock mass under tension loading. Li et al.

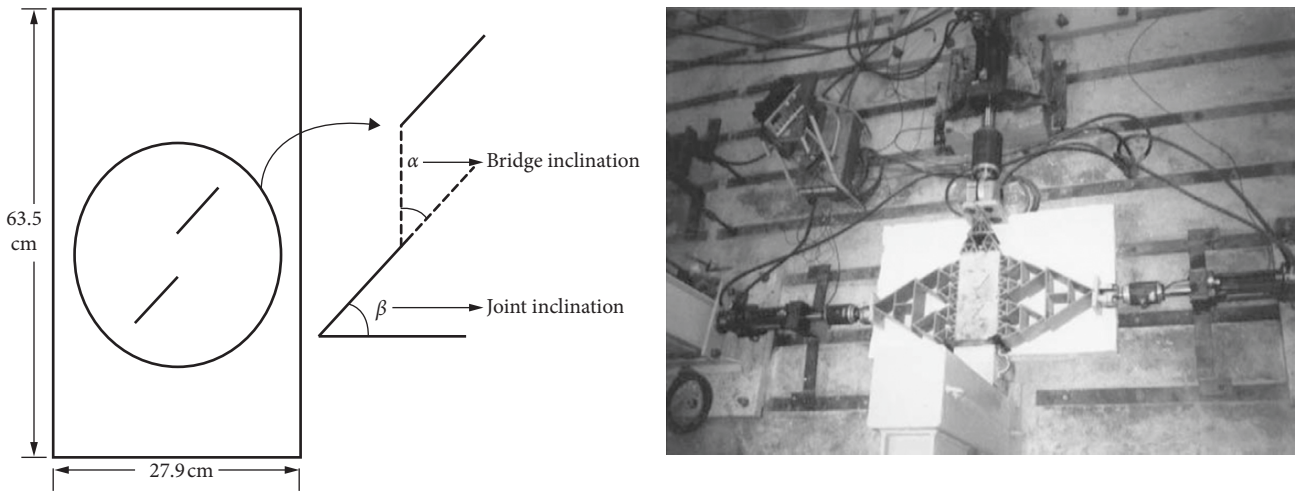

Figure 11: (a) Geometry of the specimens and (b) biaxial testing equipment setup [61].

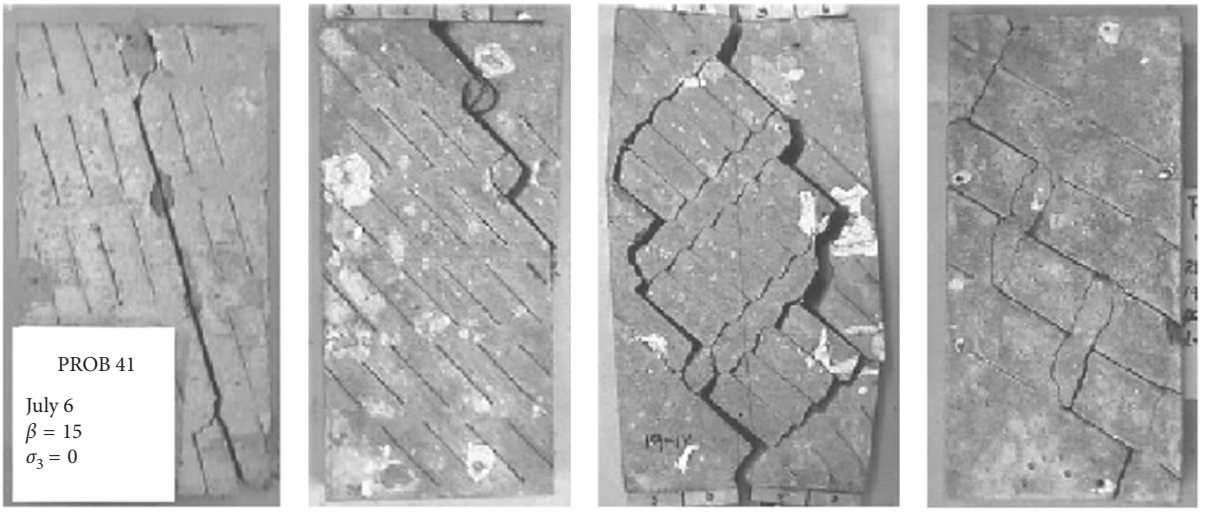

Figure 12: Observed failure modes under biaxial loading. (a) Through a plane. (b) Stepped. (c) Rotation of new blocks. (d) Interaction between rotation and stepped [52].

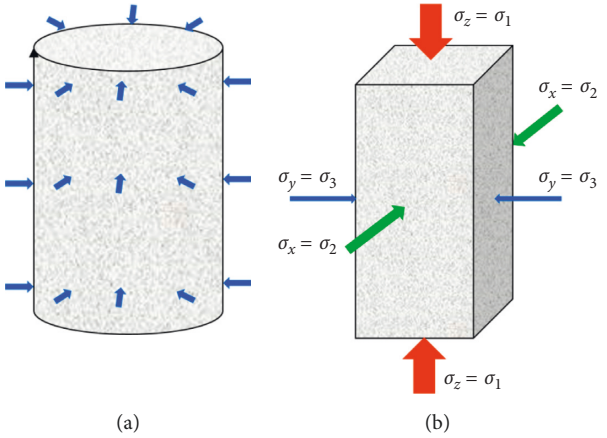

Figure 13: Two types of designs for triaxial compression tests. (a) Conventional triaxial compression. (b) True triaxial compression.

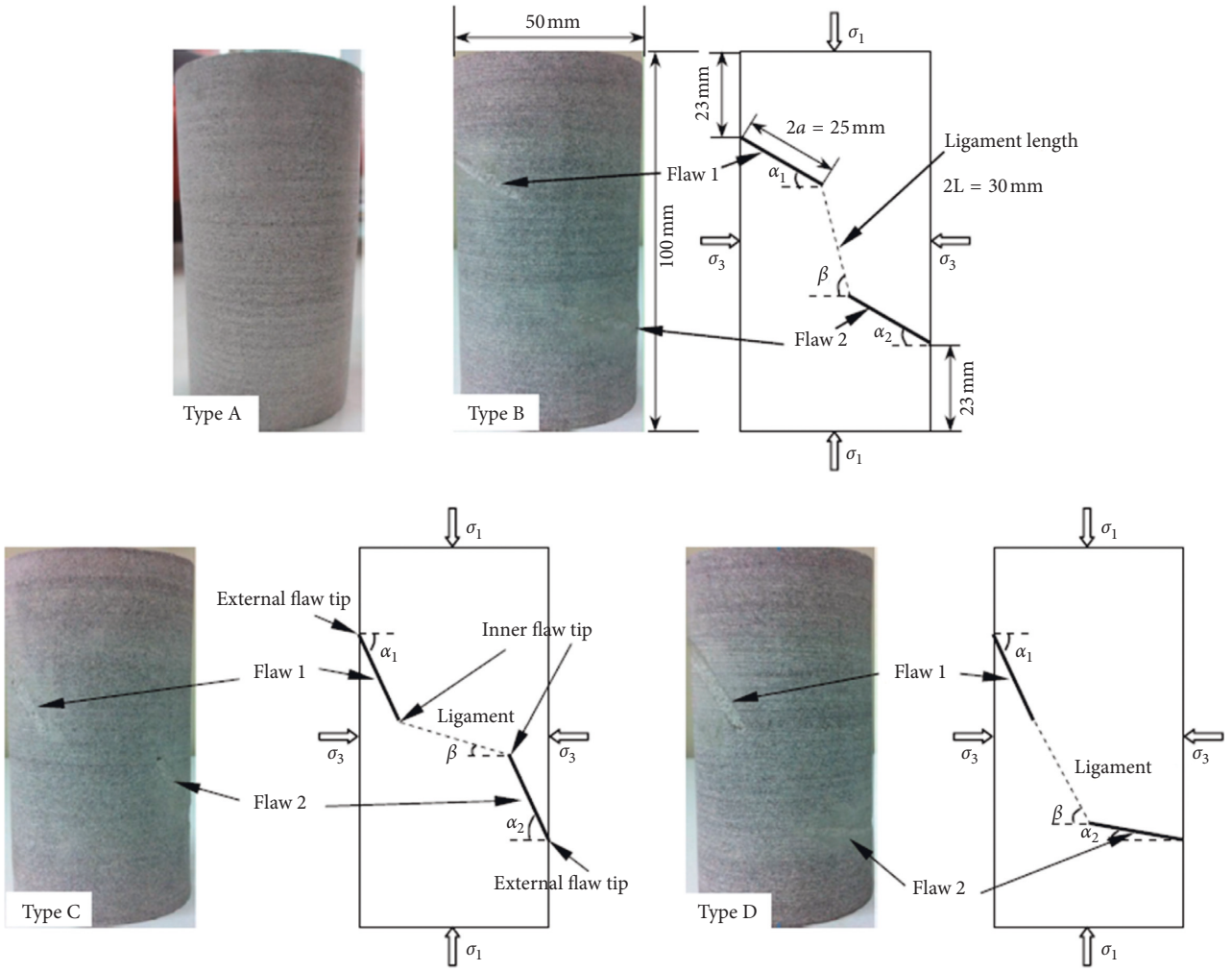

Figure 14: Four types of tested sandstone specimen and geometry of two preexisting nonoverlapping filled flaws: type A is intact specimen; types B–D are specimens with two different preexisting flaws [39].

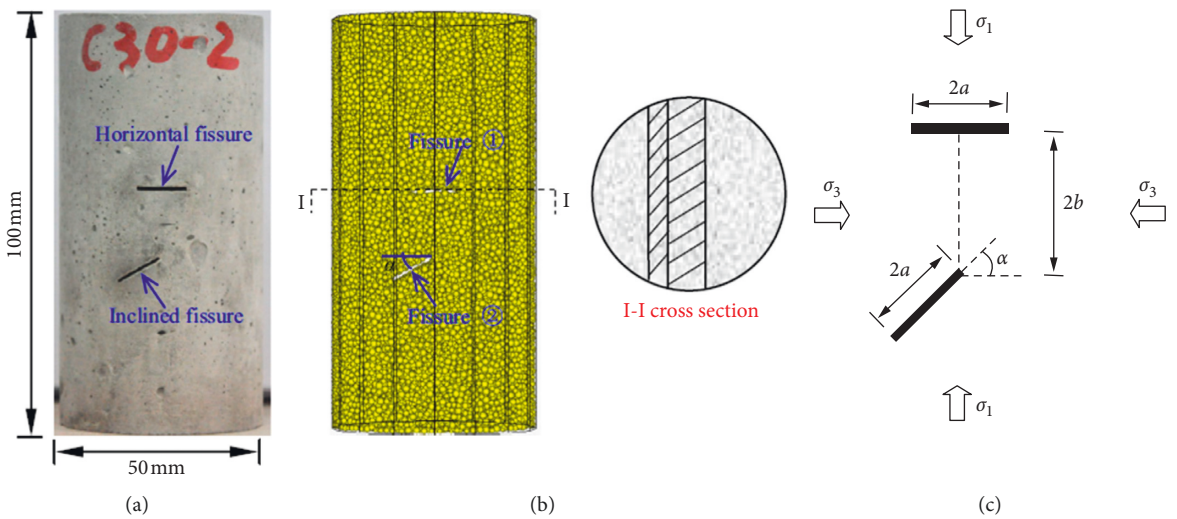

Figure 15: Specimen containing two unparallel fissures. (a) Laboratory rock-like material specimen. (b) PFC3D model and fissure surface. (c) Fissure geometry and loading condition [115].

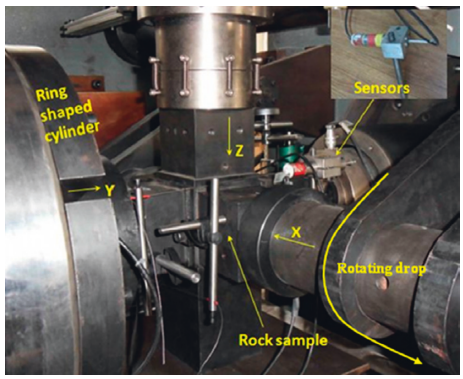

Figure 16: TRW-3000 true triaxial hydraulic servocontrolled rock test system [117].

[122] investigated the effects of loading direction on failure load and failure modes for Brazilian tests on jointed coal rock. Using a combination of experiments and numerical simulation, Haeri et al. [62] investigated the crack propagation and coalescence in rock-like disks. There are two kinds of jointed specimen made by inserting thin metal slim into the fresh mortar. For the specimen with a single crack, the width and thickness of the crack are 30 mm and 1 mm, respectively. And, the inclination of preexisting crack is 0°, 15°, 30°, 45°, 60°, and 90°. For the double-cracked specimens, the width and thickness of the crack are 20 mm and 1 mm, respectively. One crack at the horizontal, and another is oriented at different angles with respect to the horizontal (0°, 30°, 60°, and 90°). The test result shows that the crack orientation has a great influence on the failure load.In Figure 17, the failure patterns for precracked specimens under the Brazilian tensile test are shown. For the crack initiation, the fissure orientation has a significant influence on the crack initiation angle. And, the coalescence mode between the fissures is mainly tensile mode.

Compared to the indirect tension test, because of the misalignment and stress concentration during the test, the direct tension tests are difficult to perform. But, there are few people who used this method to investigate the failure behavior of jointed rocks or rock-like materials. Yang et al. [123] conducted uniaxial tension experiments on precracked rock-like specimens (Figure 18); the strength and failure behavior of specimen have been analyzed and discussed. The results indicated that crack geometry parameters including crack dip angle, crack spacing, and crack intensity, have significant influence on the strength and failure modes of the samples.

3.4. Shear Loading. As mentioned above, the crack initiation, propagation, and failure characteristics of jointed rock or rock-like specimens have been investigated by many scholars. Compared with the compressive tests, relatively few experiments were done to investigate the pattern of crack coalescence under direct shear loading [67, 68, 83, 84, 124–129]. Under shear loading, the failure behavior of jointed rock mass is different from that under compression. Lajtai [124, 125] conducted direct shear testing on rock-like specimen with nonpersistent fissures, and the test result indicated that the failure mode changes with increasing normal stress. At the same time, he also proposed a composite failure envelope to describe the changes of strength. Savilahti et al. [126] also investigated the failure behavior of jointed rock-like specimen under direct shear loading, and the influence of joint separation and overlapping on failure behavior of the jointed specimen have been analyzed. Sarfarazi et al. [67] has studied the effect of joint overlap on the full failure behavior of a rock bridge in the direct shear test via combination of the experimental test and numerical simulation. Four kinds of specimens have been tested; all of the ligament length are kept at 45 mm and the ligament angle is 0°, 25°, 90°, and 115°, respectively. During testing, the normal stress was set at 0.1 MPa, and the test results show that the failure stress decrease with increasing of the ligament angle. In Figure 19, the failure modes for specimen with different ligament angles and most of the specimen failure from the propagation of tensile crack are shown.

For the failure characteristics of the specimen with multifissures under direct shear loading, the breakage and shear behavior of intermittent joints (Figure 20) have been investigated by Gehle and Kutter [83]. The results show that the failure of specimen can be divided into three phases; both the geometrical parameters and loading conditions have been found to influence the activated shear resistance in each phase. Moreover, the mechanisms which govern the different shear phases could be identified as (1) tensile rupturing, (2) rolling and sliding friction of dilatant joint zones, and (3) sliding within the joint filling composed of brecciated material.

Apart from the direct shear loading, there is another shear test method, namely, restrictive shear test. In this loading, the compressive load and shear load on the specimen increases with the increasing of the load P. It can be used to investigate the failure process of jointed rock mass in compressive and shear environment, especially for the rock mass in rock slope. In Figure 21, the stepped failure in rock slope is shown.

Actually, there are relatively few scholars who conducted experiments to investigate the failure process of jointed rock mass under restrictive shear loading. Zhang et al. [21] has investigated the mechanical behavior of rock-like specimen mixed flaw, and the strength, fragmentation, and fractal properties have been discussed. For the mixed flaws, the length of edge-notched flaw and imbedded flaw is 10 and 30 mm, respectively. The inclination of imbedded flaw changes from 0° to 90° with an increment of 15°. Moreover, with two kinds of shear angle (45° and 60°), the jointed specimen are loaded under compressive-shear loading until failure. Based on the experimental results, three different patterns of tensile cracks and shear cracks are observed (Figure 22). At the same time, it has been found that the shear strength is a function of the flaw geometry and the shear-normal stress ratio.

3.5. Cycle Loading. Recently, for the cycle loading, most studies in the literature have focused on the mechanical behavior of intact rocks or rock-like materials under cyclic loadings. Based on the experimental tests, the hysteresis of

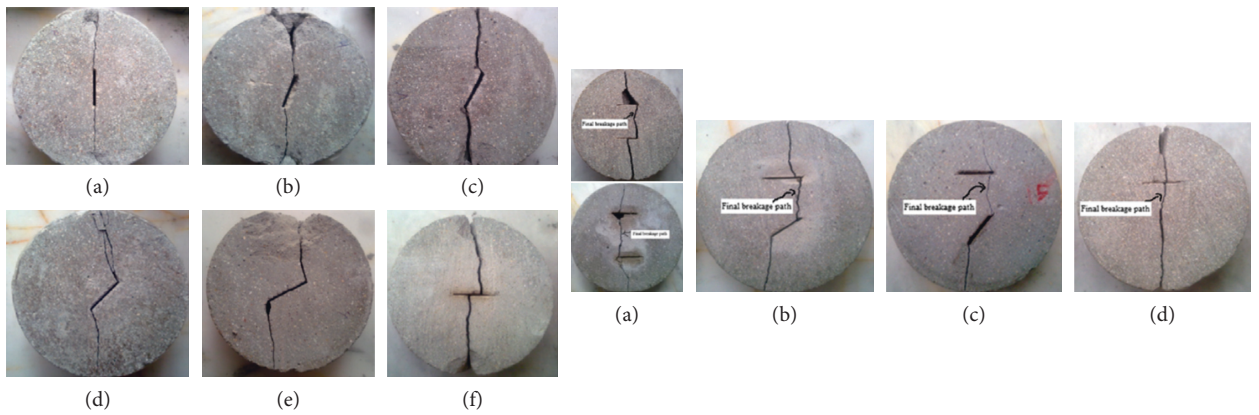

Figure 17: Experimental results illustrating the coalescence path of rock-like disk specimens containing double cracks [62].

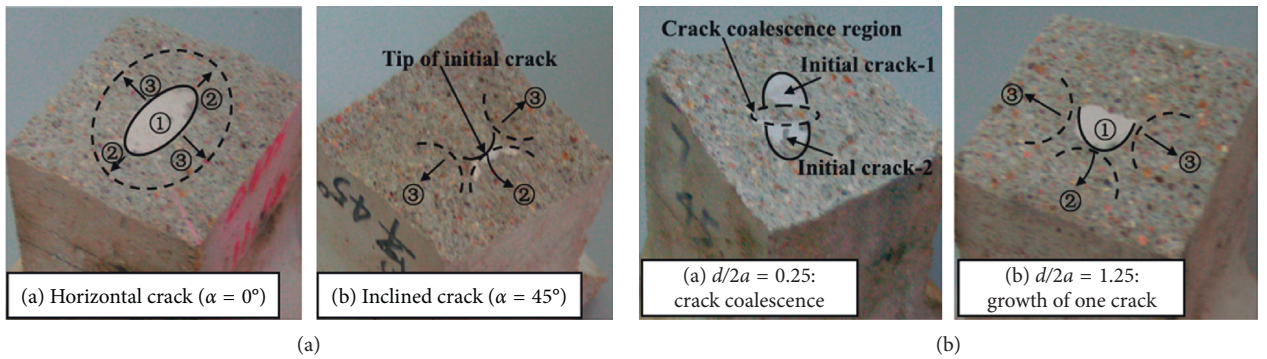

Figure 18: Failure sections of samples with single cracks: (1) initial crack; (2) wing crack; (3) lateral extension [123]. (a) Specimen with single crack. (b) Specimen with two cracks.

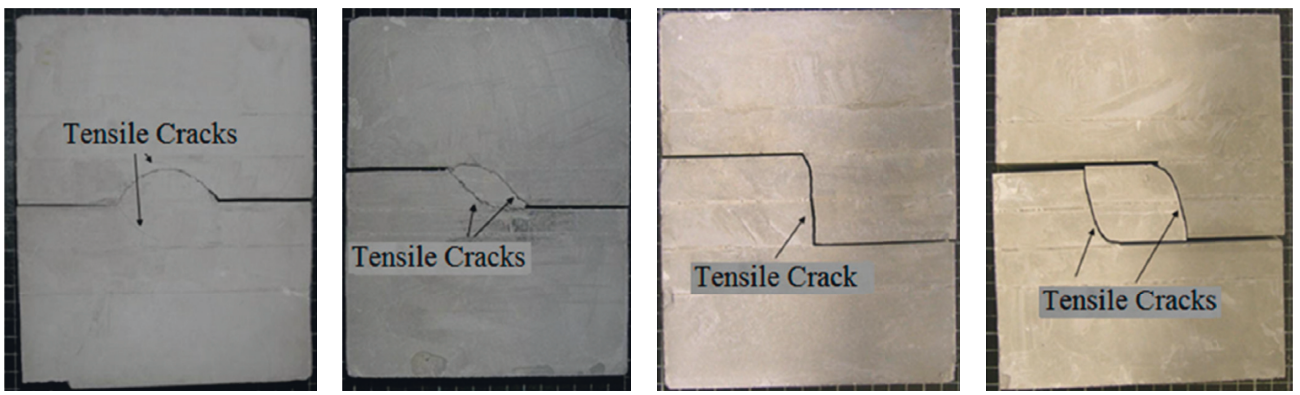

Figure 19: Crack patterns for ligament angles of (a) 0°, (b) 25°, (c) 90°, and (d) 115° [67].

the stress-strain curve has been revealed [131–134]. At the same time, the fatigue strength and deformation of the intact specimen have also been investigated by scholars, and the results indicated that the dynamic strength and elastic modulus decrease exponentially with the increase of cycles [135–139].

As mentioned above, the joint or preexisting fissure has a significant influence on the failure behavior of rock mass. The dynamic response of jointed rocks will be different from their static properties, and the mechanical behavior of jointed rock mass has also been investigated by scholars. The previous studies [140–142] reported that jointed rock mass are very sensitive to the cyclic loading and the joint confirmation has a significant influence on the dynamic strength and deformation behavior. Erarslan and Williams [143] conducted the static and cyclic loading test on inclined cracked chevron notched Brazilian disc (CCNBD) specimens, and the experimental results show that the failure load obtained through cyclic loading decreased between 30 and 45% compared with those in static loading. Liu et al.

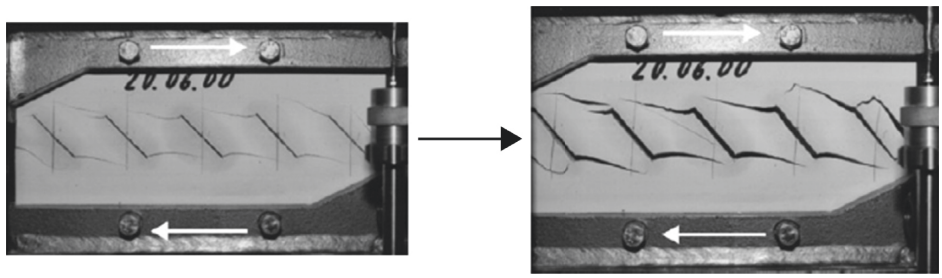

Figure 20: Rotating mechanism of the rock bridges in the second phase of shearing [83].

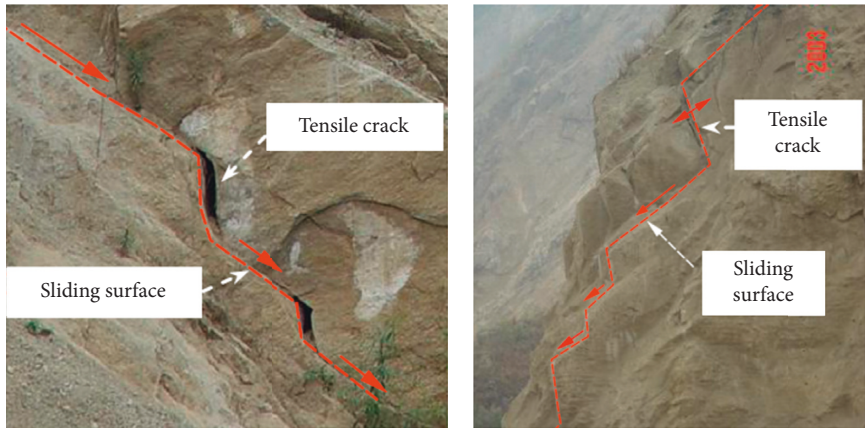

(a) (b)

Figure 21: Photographs of step-path failure in the reservoir slopes of the Xiaowan hydroelectric station, China (Huang et al. [130]).

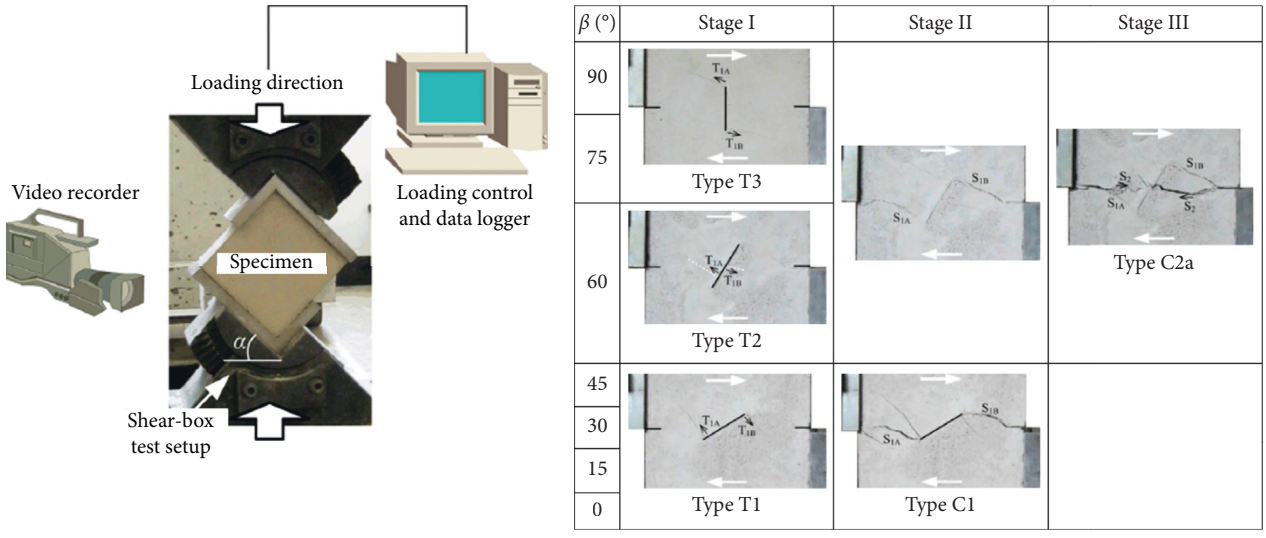

(a) (b)

Figure 22: Restrictive shear test, failure patterns, and peak shear strength of jointed specimen [21]. (a) Layout of the loading system. (b) Patterns of crack propagation and coalescence.

[63] performed the cyclic uniaxial compression test on jointed rock-like specimens, and the influence of joint geometric parameters such as dip angle, persistency, density, and spacing on mechanical properties of intermittent jointed specimen have been investigated. The test result indicated that the stress-strain curve of jointed rock under cyclic loadings is dominated by its curve under monotonic uniaxial loadings. At the same time, under cyclic loading, two types of cracks were observed in the jointed specimen. To be specific, shear cracks mainly occur in the specimen with higher joint inclination angle or higher persistency.

4. Numerical Simulation

Compared with the in situ test and laboratory test, the numerical simulation is an economical and practical method to simulate the failure process of jointed rock masses. In recent years, many numerical methods have been widely used in rock mechanics and rock engineering. These include the FEM or XFEM [144–151], DDA [152–155], NMM [156–158], smoothed particle hydrodynamics [159–162], and PFC [17, 163–172]. Overall, most of the numerical results show good agreement with experimental results.

4.1. FEM or XFEM. Based on the finite element method (FEM) and nonlinear dynamics method, Li and Wong [173] has investigated the influence of inclination angle and loading condition on crack initiation and propagation. The numerical results indicated that the loading condition has influence on crack initiation sequences and the overall crack pattern. Under a relatively low loading rate or a small magnitude of maximum loading pressure, tensile crack appears first. However, under a relatively high loading rate and a large magnitude of maximum loading pressure, shear crack would occur first (Figure 23).

For the closed fissure, Xie et al. [174] used XFEM to investigate the crack initiation and propagation in rock-like material with closed fissure under uniaxial compression. The numerical simulation results show that (1) for the specimen with inclination angles 30° and 45°, minor effects are exerted by crack surface friction on the stress distribution around the fissures, and the effect are much more obvious when inclination angle is 60° (Figure 24); (2) when the inclination angle is 45°, it is the most favorable value for crack propagation; (3) the friction seems only to play a minor role on the initiation location and angle of the wing cracks, but the friction has a great influence on the propagation length.

RFPA2D is developed by Northeastern University, People's Republic of China, and it can be used to model the evolution of damage in brittle materials by allowing the linear elastic elements to fail in a brittle manner. In recent years, this method has been used for modelling progressive failure in rocks or jointed rock-like materials. Based on RFPA2D, Tang and Kou [145] presented two particular cases concerning crack propagation and coalescence in brittle materials (the model containing a row of small flaws and several larger flaws and the model containing randomly distributed homogeneities as shown in Figure 25). The numerical results show that, under axial compression, wing crack occurs at the tips of the preexisting flaws, and propagation occurs along with the direction of maximum far-field compression. At the same time, the coalescence between preexisting flaws may be in tensile, shear, and combination of tensile/shear pattern. With a confining pressure, the crack becomes stable. However, lateral tensile stress has a significant influence on the crack growth; even a small value will result in unstable growth. For the specimen containing homogeneities on a grain scale, the numerical results indicated that the failure characteristics strongly depend on the mechanical and geometric properties of the grains and inclusions. For the failure behavior of the jointed specimen under axial compression, Tang et al. also conducted similar numerical studies through RFPA2D, such as crack coalescence in rock-like materials containing three flaws [108]; the numerical results also show qualitatively a reasonably good agreement with reported experimental results. Wong et al. [175] conducted numerical simulation by using RFPA2D to investigate the splitting failure in brittle rocks containing open joints under uniaxial compressive loading. And, the influence of preexisting joint length on wing crack growth has been studied.

Apart from the axial compression, RFPA2D can also be used to investigate the failure process of the jointed specimen under shear loading. Zhang et al. [176] has investigated the shear behavior of rock specimens with several intermittent joints (Figure 26). Based on the numerical simulation, the whole failure process and the failure patterns are observed. For the failure pattern under shear loading, it is mostly affected by joint geometry parameters, and the shear strength of the specimen is related to the failure pattern. Moreover, both the joint separation and azimuth angle have influence on the wing crack propagation, and the wing crack dominates the overall failure of the specimen. Furthermore, the results also show that the macroshear crack is the result from the accumulation of microtensile damage.

Da Huang et al. [31] used the ANSYS AUTODYN-2D and investigated the crack initiation and propagation in three types of precracked sandstone specimens under conventional triaxial compression. In Figure 27, the comparison between numerical and experimental results is shown. The coalescence pattern in numerical results shows a great agreement with that in experimental results. The result also indicated that the crack initiation stress, critical stress of dilation, and peak strength for precracked specimens are far below than those in intact rocks. At the same time, all of them increase with the confining pressure.

4.2. DEM. In recent years, the DEM has been widely used by scholars to model the failure process of the jointed rocks or brittle rock-like materials. DEM has experienced decades of development, and many kinds of DEM software have sprung up in recent years, such as PFC2D/3D, UDEC, and 3DEC. For crack initiation and propagation, the PFC has been widely accepted by scholars, and the numerical results show a great agreement with the experimental results.

Based on the parallel bond model in PFC2D, Zhang et al. [177] has investigated the crack initiation and propagation under uniaxial compressive loading. The numerical simulation result shows that the inclination of joint has a strong influence on the crack initiation and propagation behavior. And, by analyzing the parallel bond forces and displacement fields, the crack initiation location has been identified. Moreover, two types of displacement fields, namely, type I (DF_I) and type II (DF_II), have been proposed to distinguish the tensile crack and shear crack (Figure 28). In Figure 19, two displacement field types associated with different microcracking processes are shown. For the type I (DF_I), if the two displacement trend lines diverged from each other and there

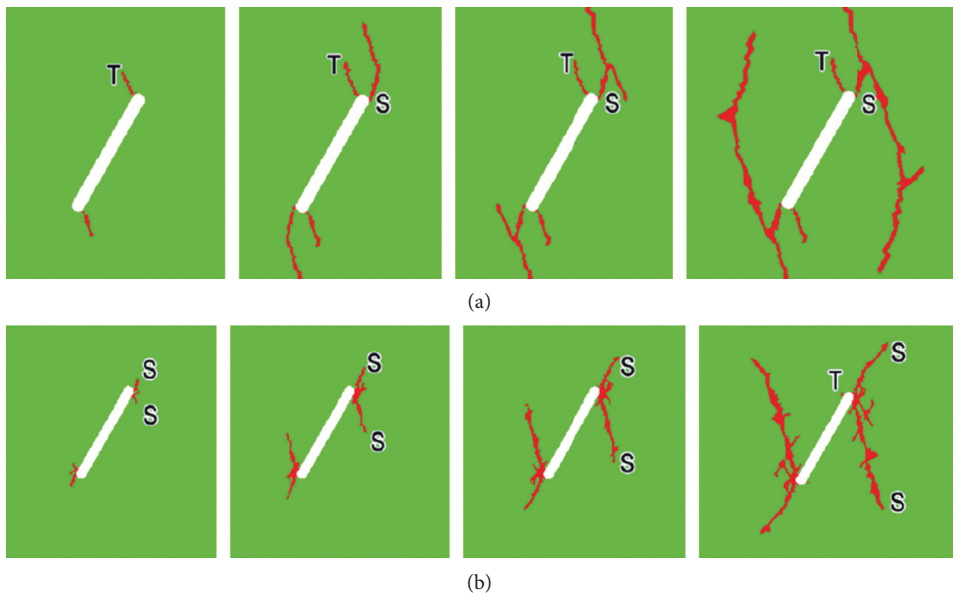

Figure 23: Initiation and propagation of cracks under different loading rates [173]. (a) A relatively low loading rate. (b) A high loading rate.

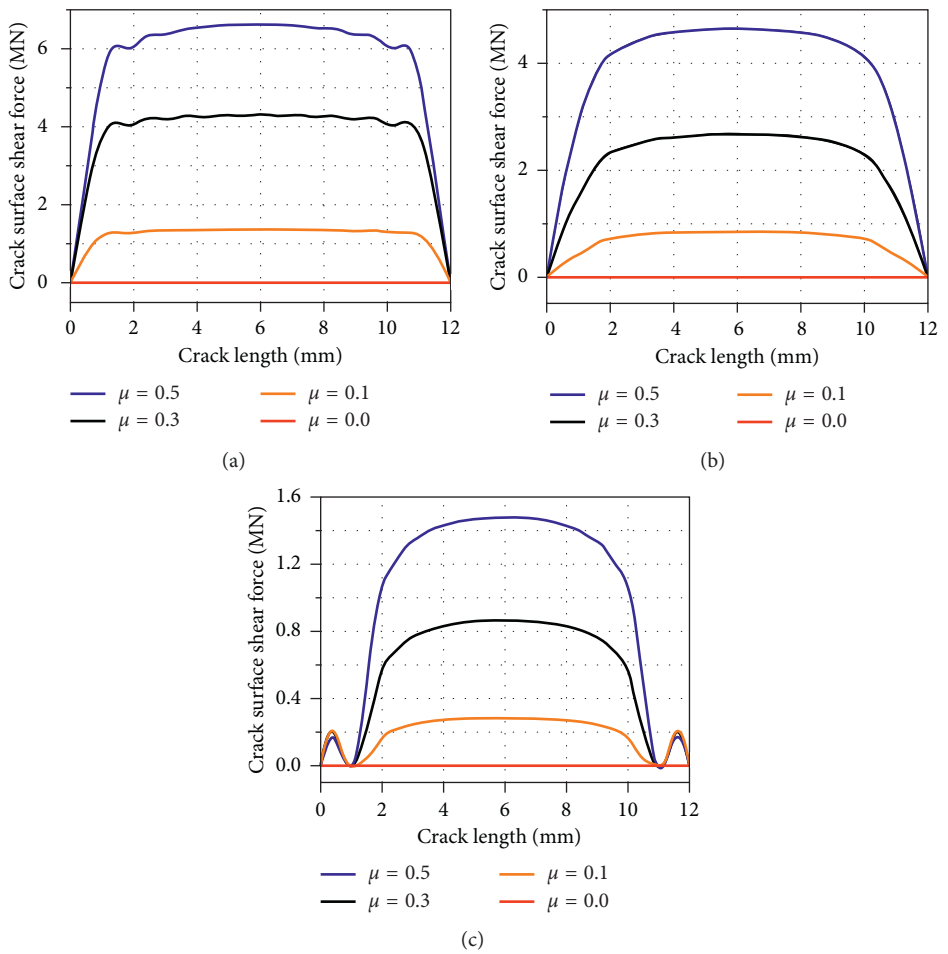

Figure 24: Crack surface shear force. Flaw inclination angle: (a) 30°; (b) 45°; (c) 60° [174].

was very limited relative shear movement, relative tensile displacement occurred dominantly in the region in between. For the type II (DF_I), if the two displacement trend lines exhibited both a relative tensile displacement and a shear displacement in the region in between. Based on the parallel bond model, the crack initiation, propagation, and

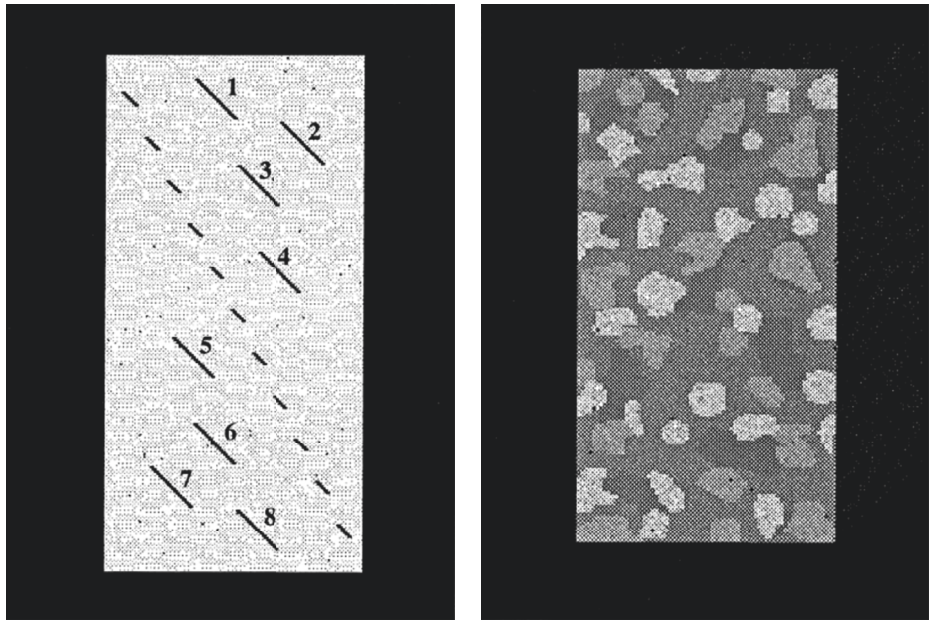

(a) (b)

Figure 25: The numerical models for the simulations. Model containing (a) a row of small flaws and several larger flaws and (b) randomly distributed homogeneities [145].

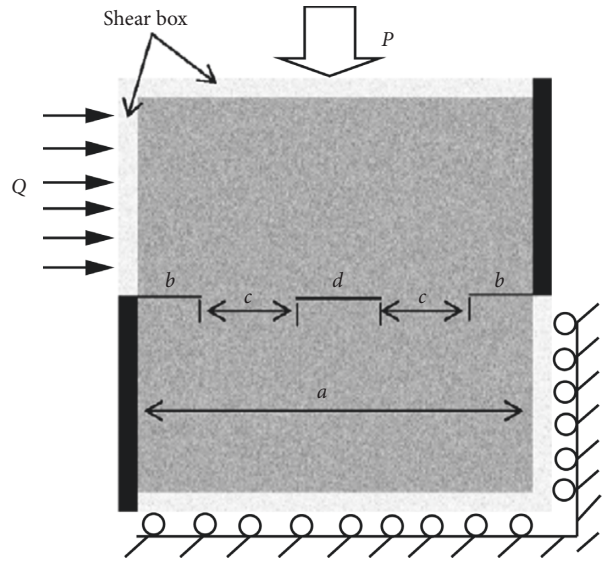

Figure 26: The example of numerical specimen under direct shear loading condition (Zhang et al.) [176].

coalescence in between two fissures have been further investigated by Zhang et al. [111]. Lee and Jeon [17] have investigated the crack initiation, propagation, and coalescence between unparallel fissures under uniaxial compression. The relationship between crack initiation, coalescence, and failure stress and fissure inclination angle in the single and double crack has been analysed.

Apart from the specimen with open or closed fissure, the failure characteristic of multifissure specimen has also been extensively discussed in literatures. Cao et al. [53] used the PFC2D to model the failure behavior of multifissure specimen under uniaxial compression, and the fissure geometry parameters such as inclination (α) and fusser number (N_f) have been taken into consideration. Based on the numerical results, the influence of fissure geometry on peak strength of multifissure specimen has been discussed. To be specific, the peak strength increased with increasing of inclination angle. The material strength was lowest for inclination angle 25°, and highest for 90°. The influence of N_f on the peak strength depended on α. For $\alpha = 25°$ and 45°, N_f had a strong effect on the peak strength, while for higher α values, especially for the 90° sample, there were no obvious changes in peak strength with different N_f values. At the same time, the failure modes in the simulated results also agree very well with those in experimental results.

Fan et al. [172] usd the PFC3D to investigate the macromechanical behavior of jointed blocks with multinonpersistent joints under uniaxial loading (Figure 29). The effect of joint inclination, size, and joint mechanical properties on the strength, deformability, stress-strain, and failure modes have been studied. The simulation results indicated that the joint particle stiffness only play a minor to a significant role on peak strength depending on inclination and joint density. And, the joint particle stiffness plays a negligible role on deformation modulus depending on inclination and joint density value. For the stress-strain curves, they can be further classified into four types. Moreover, the failure modes such as (1) splitting failure; (2) plane failure; (3) stepped path; and (4) intact material failure occurring in numerical results also agree well with those in experimental results.

By use of numerical direct shear tests (PFC2D), Sarfarazi et al. [67] has investigated the effect of joint overlap on the failure process of the jointed specimen. In Figure 30, the planar nonpersistent joints and en echelon

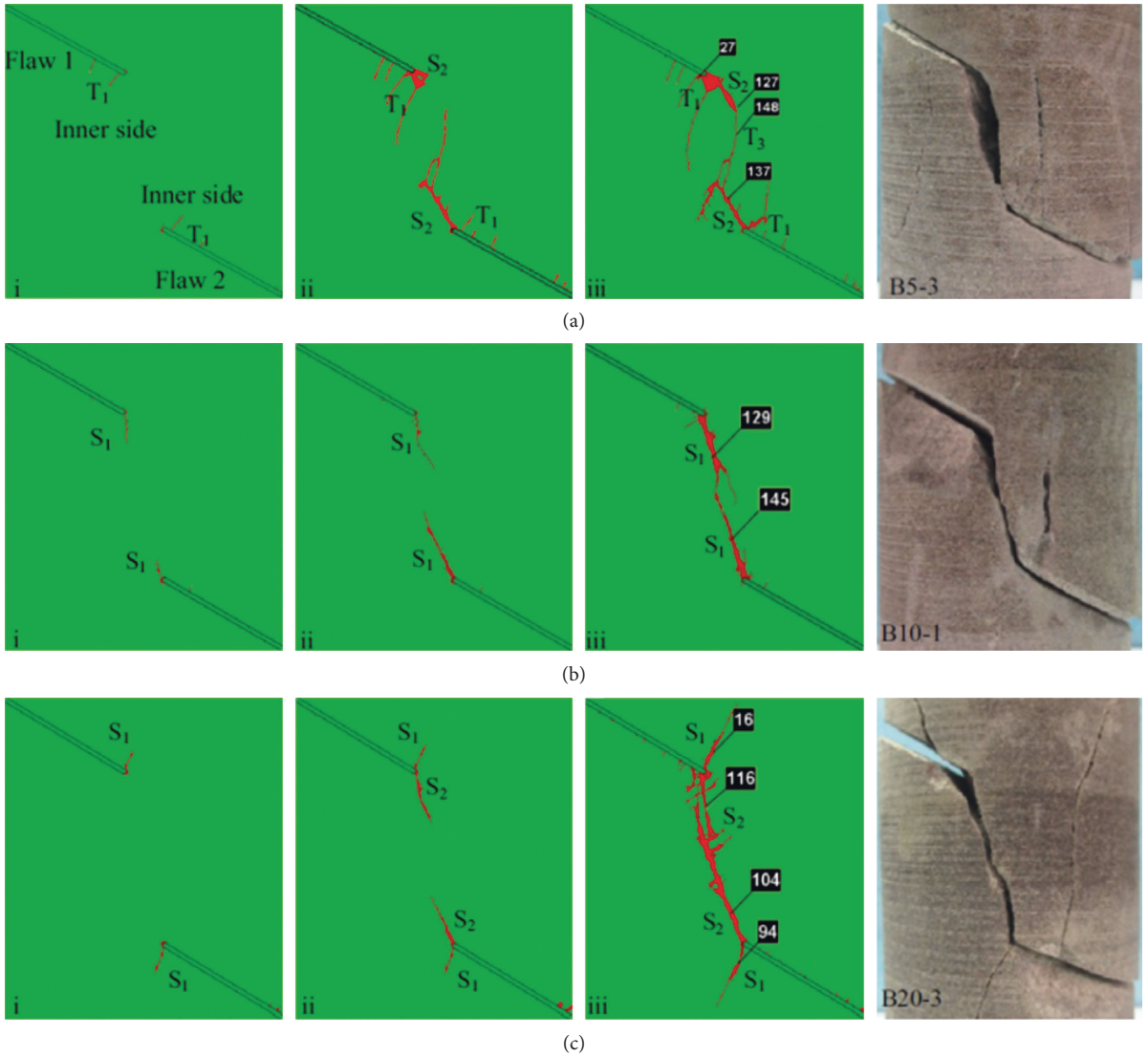

Figure 27: Comparison between numerical (ANSYS AUTODYN-2D) and experimental results [39].

nonpersistent joints in the numerical specimen are shown. The ligament angle is 0°, 25°, 90°, 115°, and 140°, and the ligament length is kept constant for all specimens (18 mm). Moreover, the lengths of the edge-notched joints are 21, 21.8, 24.2, 33.8, and 36.9 mm for ligament angles of 0°, 25°, 50°, 90°, 115°, and 140°, respectively. The simulation results indicated that the rock bridge lost their capacity when nearly 50 % of total cracks developed within the rock bridge. Furthermore, the simulation results also show that the macroshear failure in rock-bridge results from the cluster of microtensile cracks.

Based on the discrete element software UDEC, Vergara et al. [178] studied the mechanical behavior of rock containing parallel nonpersistent joint (Figure 31). And, the results indicated the large anisotropy in the strength resulting from variation of the joint orientation and lower strength of the specimens was caused by the coalescence of fractures belonging to parallel joint sets.

Jin et al. [179] used 3DEC software to simulate the anisotropic mechanical behaviors of columnar jointed basalt under compression (Figure 32). The results show that, with different primary joint angles, the jointed specimen exhibits different mechanical properties under the presence of confining pressure. The primary joints play an important role on the anisotropy of the jointed specimen. At the same time, it is found that increasing confining pressure can reduce the influence of columnar joints on the anisotropy of mechanical properties obviously.

4.3. FEM-DEM. As a kind of heterogeneity material, natural rocks containing fracture and the fragmentation processes limit the applicability of continuum-based models to model the failure behavior of natural rock mass in rock engineering. In order to resolve or improve these limitations, Munjiza et al. [180] proposed the finite-discrete element method (FEM-DEM). For the FEM-DEM method, the discrete element has been discretised into finite elements. It is indicated that there is a finite element mesh associated with each discrete element. Then, the

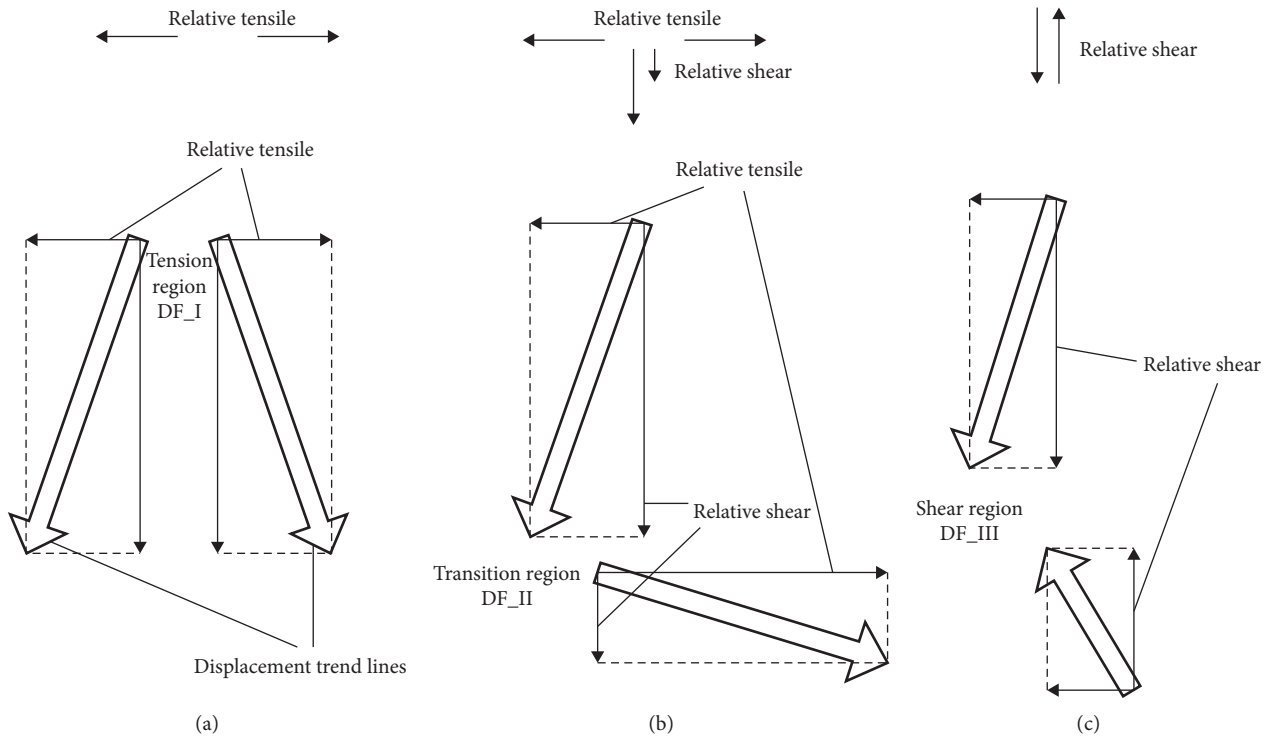

Figure 28: Three displacement field types defined by displacement trend lines. (a) Type I displacement field (DF_I). (b) Type II displacement field (DF_II). (c) Type III displacement field (DF_III) [177].

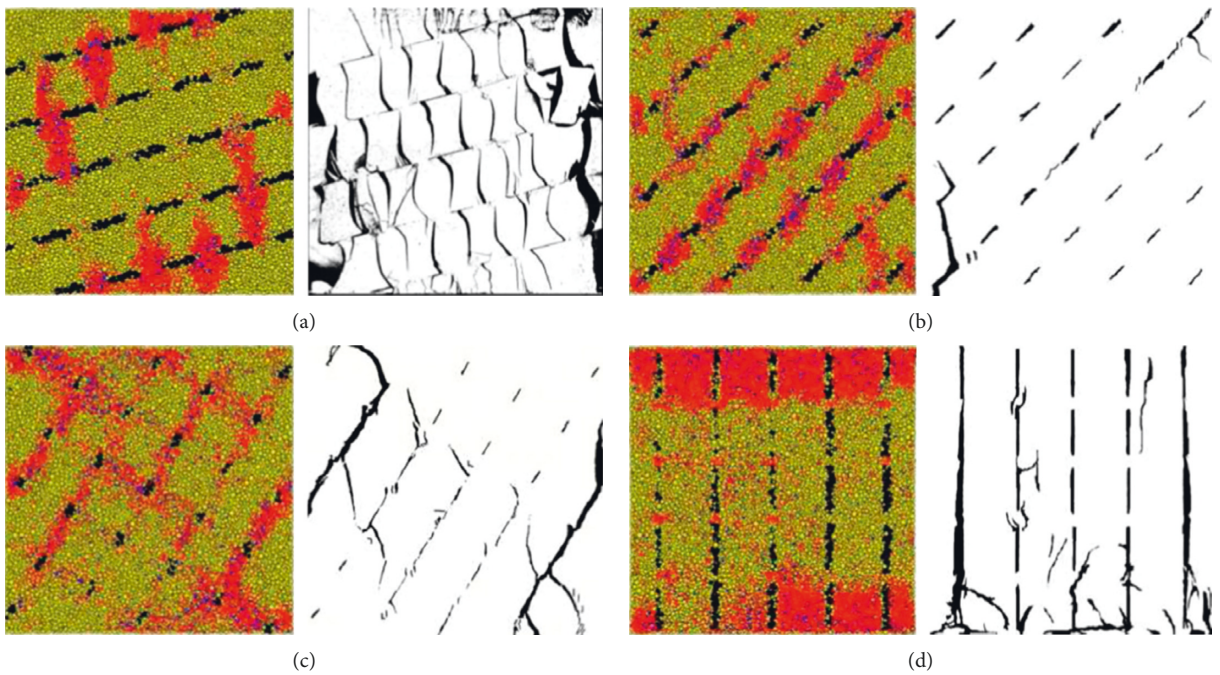

Figure 29: Failure mode comparisons between experimental and numerical results. (a) Splitting failure mode. (b) Plane failure mode. (c) Step-path failure mode. (d) Intact material failure mode [172].

continuum behavior is calculated through finite elements, and discontinuum behavior is considered based on discrete elements. The FEM-DEM method has also been used by scholars to investigate the failure process of jointed rocks under different kinds of loading conditions [181–184].

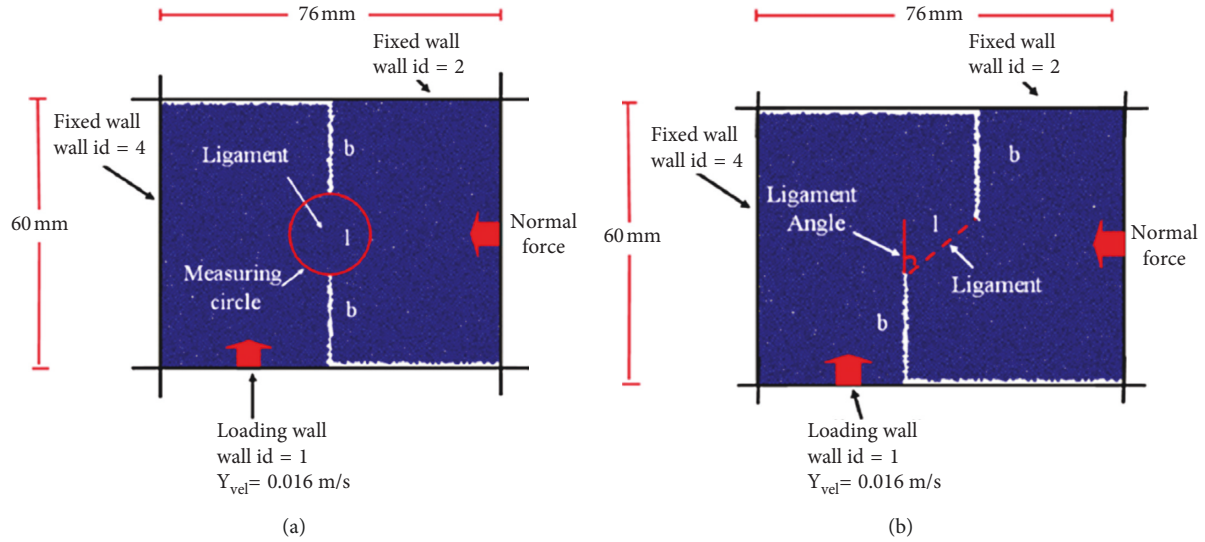

Figure 30: (a) Planar nonpersistent joints and (b) en echelon nonpersistent joints [67].

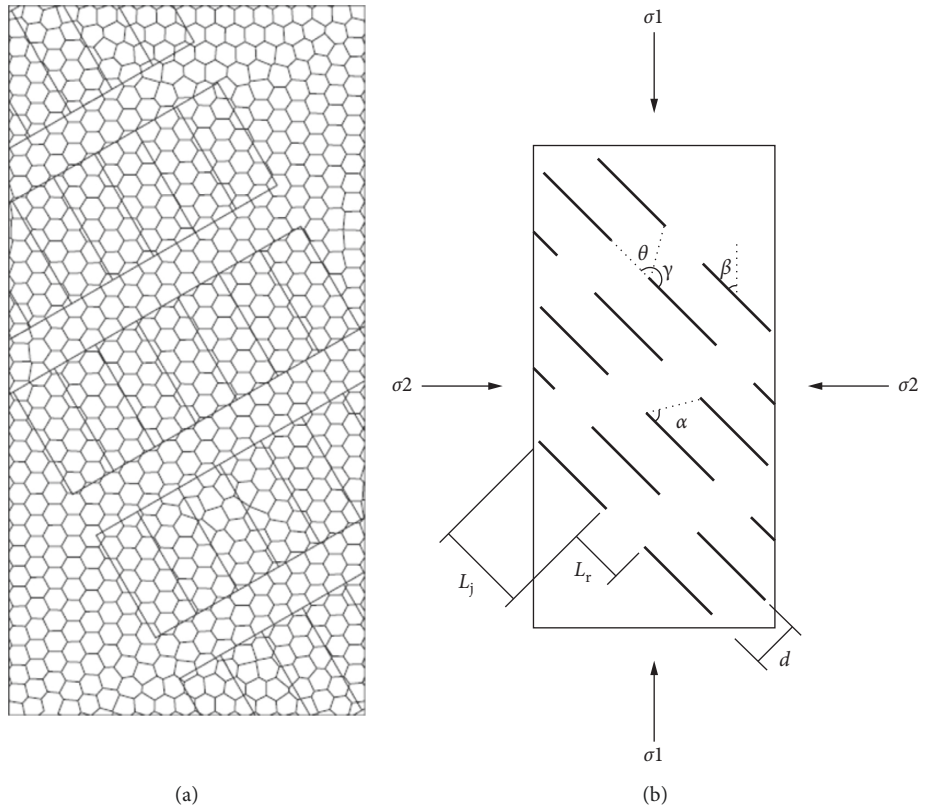

Figure 31: (a) Specimen modeled with UDEC including fictitious and preexisting (nonpersistent) joints with $\beta = 30^{\circ}$. (b) Geometrical parameters of the nonpersistent joints and direction of the principal stresses [178].

For example, Lisjak et al. [182] used the finite-discrete element method (FEM/DEM) to model the mechanical behavior of layered materials (Figure 33), and the results also demonstrated the effectiveness of the finite-discrete element method in simulating the short-term mechanical response of the Opalinus clay.

4.4. Other Numerical Methods. The Fast Lagrangian Analysis of Continua 3D (FLAC3D) has also been used by scholars to investigate the crack initiation and propagation in jointed rocks or rock-like materials [98, 185–188]. For example, based on the FLAC3D, Fu et al. [98] proposed a new kind of elastic-brittle model to model the crack initiation and

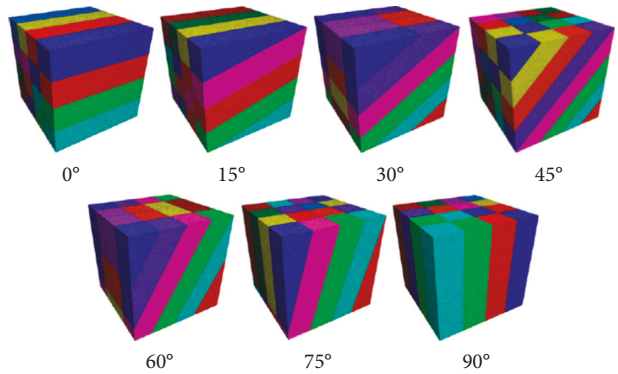

Figure 32: 3DEC models of columnar jointed basalt with different joint dip angles [179].

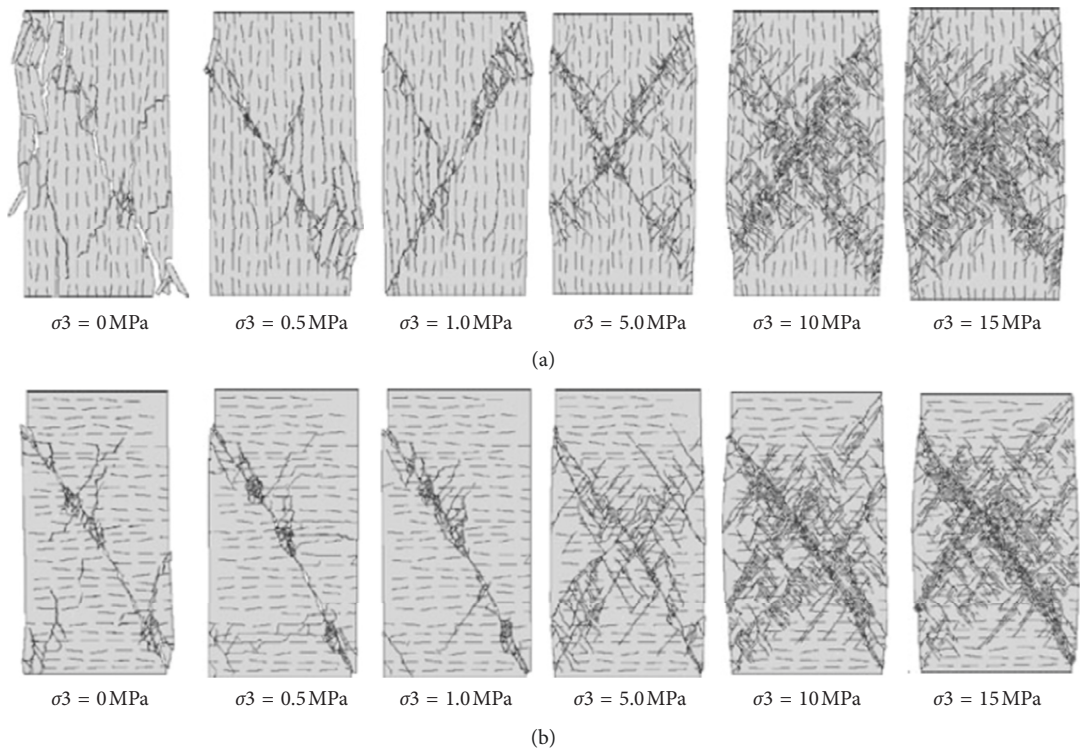

Figure 33: Simulated fracture patterns of the (a) P-sample and (b) S-sample for increasing confining pressure values [182].

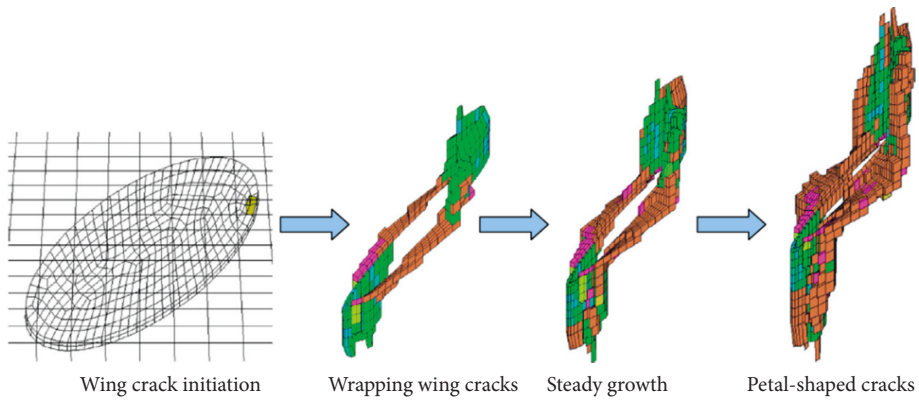

Figure 34: Continued.

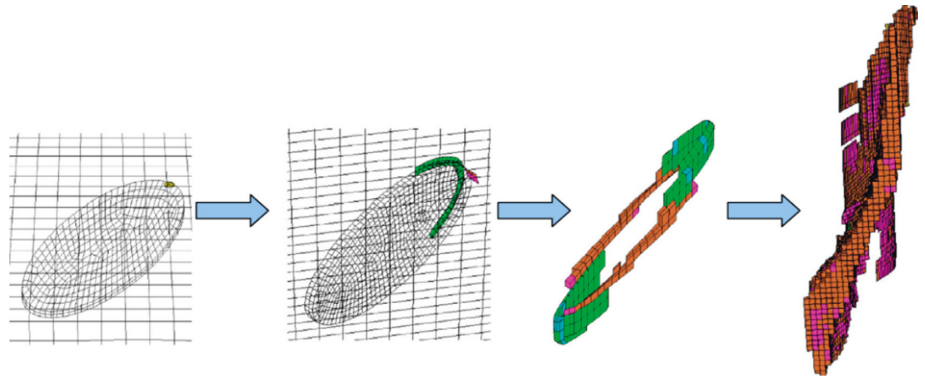

Figure 34: 3D views of the crack propagation process under uniaxial (a) and biaxial (b) loading [98].

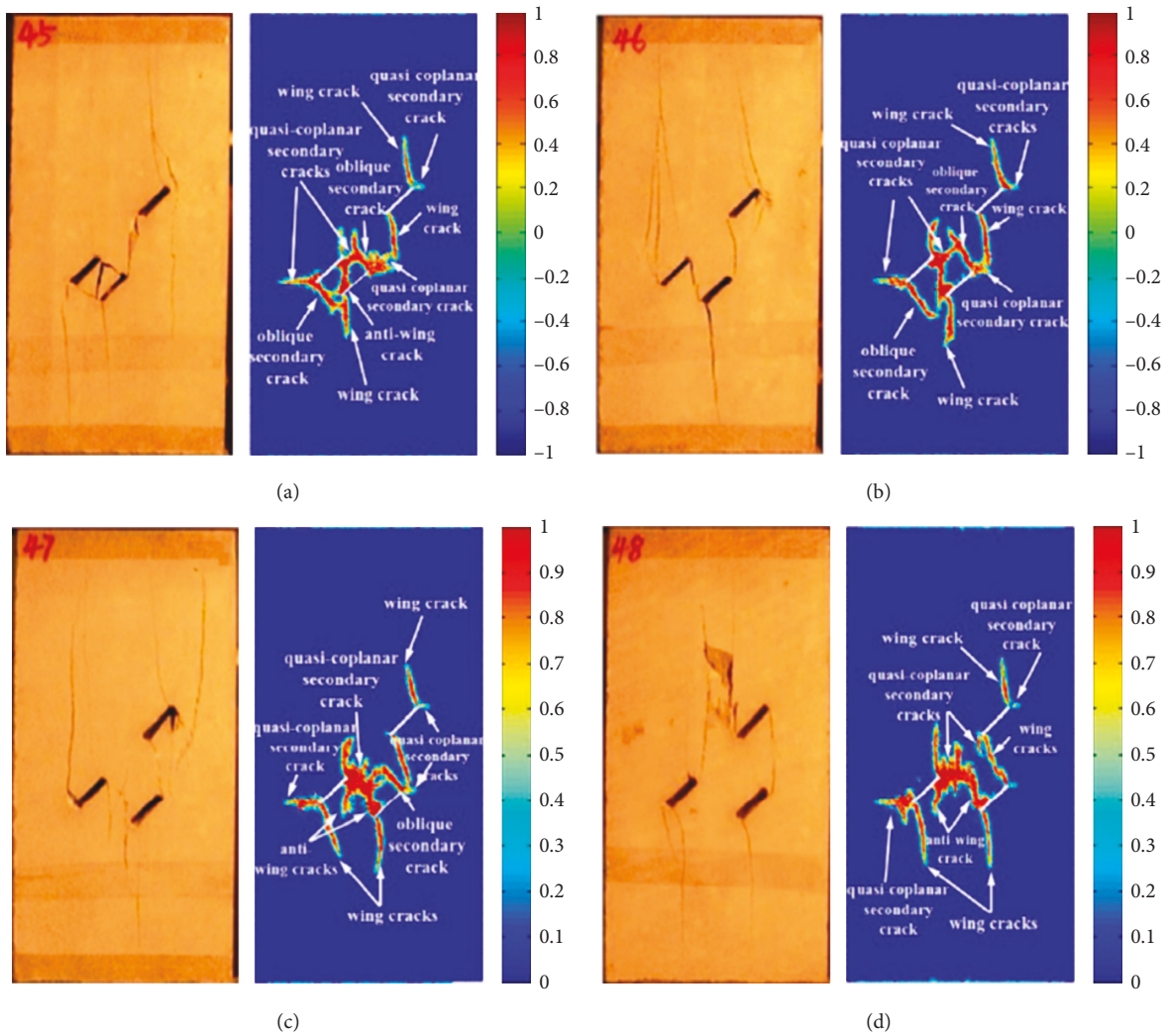

Figure 35: Comparison of crack growth paths in the sandstone samples containing three preexisting flaws with the different ligament angle β_2 obtained from the proposed numerical method and the previous experimental results [29]. (a) 75°. (b) 90°. (c) 105°. (d) 120° [189].

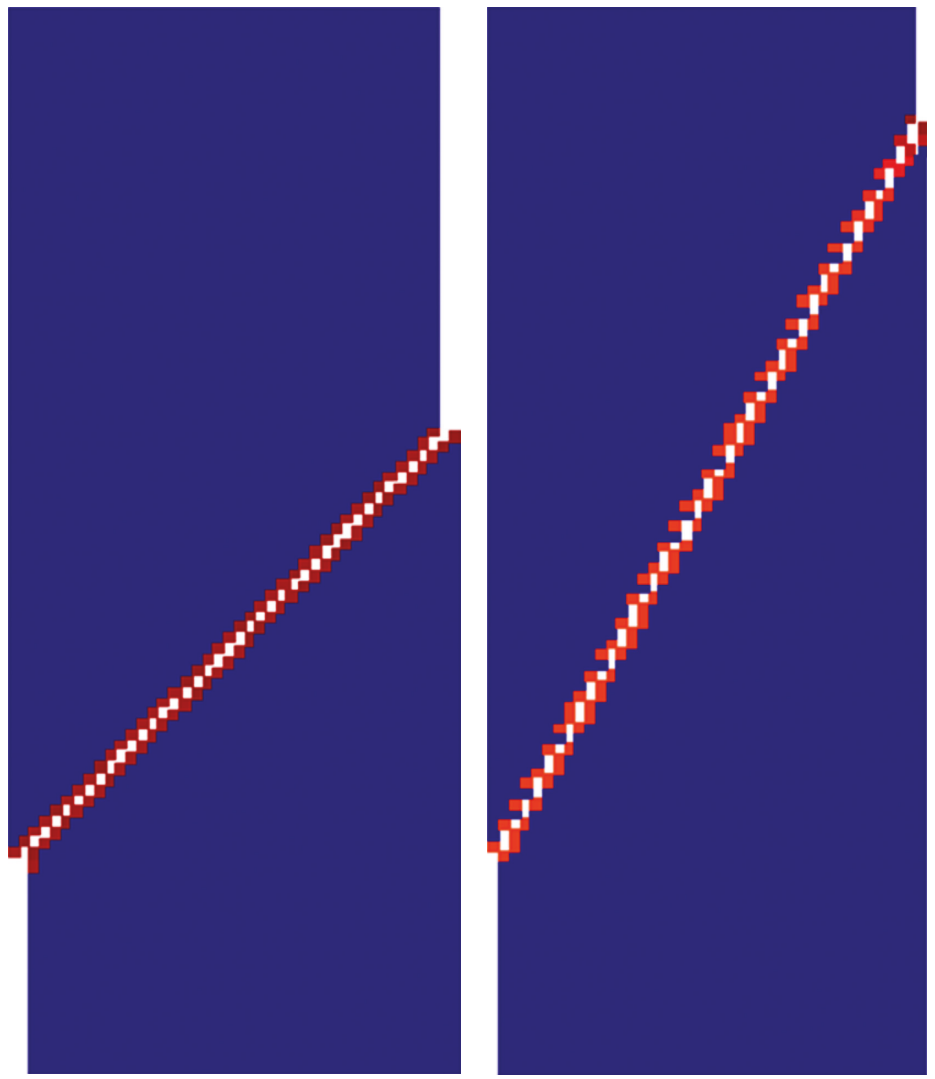

Figure 36: Accumulated plastic strain in the postfailure process for (a) $\theta = 45^{\circ}$ and (b) $\theta = 60^{\circ}$ [161].

propagation of 3D fissure. The uniaxial and biaxial numerical results show an excellent consistency with experiment results. In Figures 34(a) and 34(b), the 3D views of the crack propagation process under uniaxial loading and biaxial loading, respectively, are shown. To be specific, under uniaxial loading, secondary cracks are all wing cracks and formed at both ends of the precrack's major axis. Under biaxial loading, (the lateral stress is 20% of the peak stress), a few antiwing cracks appear. Accordingly, only in high lateral stress, antiwing cracks will appear.

Combined with maximum tensile stress criterion and the Mohr–Coulomb criterion, the extended nonordinary state-based peridynamics has been used for modelling the initiation, propagation, and coalescence of the jointed rocks under compressive loads by Wang et al. [189–196]. Different types of cracks includes wing crack, oblique secondary crack, quasi-coplanar secondary crack, and antiwing crack are modeled and distinguished by the proposed method, and the numerical results show a great agreement with the previous experimental ones (Figure 35).

Pramanik and Deb et al. [161] used a kind of methodology which is developed in the SPH framework to investigate the failure behavior of rock material containing multiple discontinuities or joints. In this method, the joint is represented by a set of particles at the location of the joints. At the same time, based on the Drucker–Prager yield criterion, the free-sip, no-sip, and symmetric boundary conditions are also implemented in this method. In Figure 36 the failure mode of the specimen with different joint inclination is shown, and the numerical results are in good agreement with derived theoretical results. The efficacy of the numerical method is successfully demonstrated by two samples under uniaxial and gravitational loading conditions. Moreover, this method also has shown promises to model the failure process of jointed rock mass in three dimensions. For this kind of method, more examples have been discussed in previous works [159–162].

Yao et al. [197] proposed an extended rigid block spring method (RBSM) to model the damage and failure of anisotropic rock mass. In this method, the tensile failure

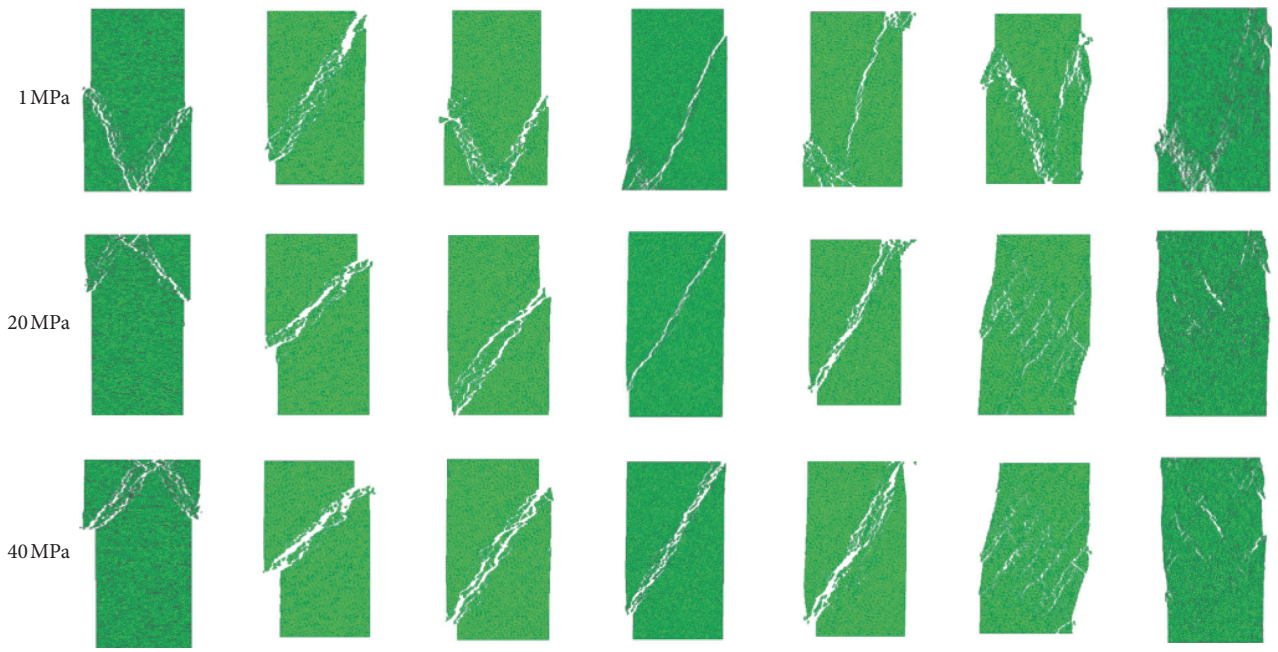

Figure 37: Failure modes for specimens with various orientations under compression with different confining pressures [197].

between interface occurs when normal stress reaches the tensile strength. However, the shear failure is described by a nonlinear criterion in terms of the local normal and shear stresses. In Figure 37, the failure modes of rock mass under different confining pressure are shown. The numerical results indicated that the inherent bedding plane and confining pressure have a significant influence on the macroscopic mechanical strength and failure mode of rock mass. In addition, the numerical results agree well with typical experimental data for both elastic properties and mechanical strength. Meng et al. [198–201] formulated a series of discrete numerical mechanics models as standard second-order cone programs. Advanced optimisation algorithms can be employed to solve the problem. It is necessary to note that the purely static discrete element method can be employed. Furthermore, both the hard-sphere and soft-sphere discrete numerical models can be recovered.

Notably, apart from the numerical methods mentioned above, there are also other methods developed by scholars and been used to model the failure process of rocks or rock-like materials. However, they cannot be listed all here one by one.

5. Conclusion

The discontinuities have a great influence on the mechanical behavior of rock mass, and under loading, the failure of natural rock mass results from the crack propagation and coalescence in rock mass. Compared with the intact rocks, the jointed or fractured rock mass usually exhibits weaker and highly anisotropic mechanical characteristics.

The experimental results indicated that the joint confirmation parameters have a significant influence on the mechanical behavior of rock mass. The strength parameters of jointed rocks decrease with the increasing of joint number, length, and persistent degree. At the same time, the strength of the jointed rocks usually has the lowest value when inclination is around 45°. For the failure characteristics of jointed rocks, the coalescence between joints includes tensile, shear, and mixed modes.

The numerical simulation has been viewed as a kind of economical and practical method and has also been accepted by many scholars. Compared with FEM or XFEM, the DEM exhibits strong advantage in crack initiation and propagation. In recent years, the DEM has been widely used to model the failure behavior of jointed rocks or rock-like materials, and most of the numerical values are in good agreement with experimental results. Moreover, other kinds of numerical methods such as NMM, smoothed-particle hydrodynamics, peridynamics, and RBSM have also been successfully applied to the analysis of failure process of jointed rocks.

Conflicts of Interest

The authors declare that they have no conflicts of interest.

Acknowledgments

This paper received funding from projects supported by the National Natural Science Foundation of China (Nos. 11772358, 51774322, and 51474249), Hunan Provincial Natural Science Foundation of China (2018JJ2500), Open Fund of Engineering Laboratory of Spatial Information Technology of Highway Geological Disaster Early Warning in Hunan Province (Changsha University of Science & Technology) (Nos. kfj70603, kfj170407, and kfj170406), and Natural Science Basic Research Plan in Shaanxi Province of China (2018JQ4015). The authors wish to acknowledge these supports.

References

[1] H. Wang, H. Lin, and P. Cao, "Correlation of UCS rating with Schmidt Hammer surface Hardness for rock mass classification," *Rock Mechanics and Rock Engineering*, vol. 50, pp. 195–203, 2016.

[2] Y. Chen and H. Lin, "Consistency analysis of Hoek-Brown and equivalent Mohr-coulomb parameters in calculating slope safety factor," *Bulletin of Engineering Geology and the Environment*, vol. 2, pp. 1–13, 2018.

[3] Y. X. Wang, P. P. Guo, W. X. Ren et al., "Laboratory investigation on strength characteristics of expansive soil treated with jute fiber reinforcement," *International Journal of Geomechanics*, vol. 17, no. 11, pp. 1–12, 2017.

[4] Y. X. Wang, P. P. Guo, F. Dai, X. Li, Y. L. Zhao, and Y. Liu, "Behavior and modeling of fiber-reinforced clay under triaxial compression by combining the superposition method with the energy-based homogenization technique," *International Journal of Geomechanics*, vol. 18, pp. 1–16, 2018.

[5] T. Liu, P. Cao, and H. Lin, "Damage and fracture evolution of hydraulic fracturing in compression-shear rock cracks," *Theoretical and Applied Fracture Mechanics*, vol. 74, pp. 55–63, 2014.

[6] G. S. Esterhuizen, D. R. Dolinar, and J. L. Ellenberger, "Pillar strength in underground stone mines in the United States," *International Journal of Rock Mechanics and Mining Sciences*, vol. 48, pp. 42–50, 2011.

[7] E. Hoek and Z. T. Bieniawski, "Brittle fracture propagation in rock under compression," *International Journal of Fracture*, vol. 1, no. 3, pp. 137–155, 1965.

[8] E. G. Bombolakis, "Photoelastic study of initial stages of brittle fracture in compression," *Tectonophysics*, vol. 6, no. 6, pp. 461–473, 1968.

[9] N. S. Park, *Crack Propagation and Coalescence in Rock Under Uniaxial Compression*, Master's Thesis, Seoul National University, 2001.

[10] B. Shen, "The mechanism of fracture coalescence in compression-experimental study and numerical simulation," *Engineering Fracture Mechanics*, vol. 51, no. 1, pp. 73–85, 1995.

[11] A. Bobet and H. H. Einstein, "Fracture coalescence in rock-type materials under uniaxial and biaxial compression," *International Journal of Rock Mechanics and Mining Sciences*, vol. 35, no. 7, pp. 863–888, 1998.

[12] A. Bobet and H. H. Einstein, "Numerical modeling of fracture coalescence in a model rock material," *International Journal of Fracture*, vol. 92, no. 3, pp. 221–252, 1998.

[13] O. Reyes and H. H. Einstein, "Failure mechanisms of fractured rock-A fracture coalescence model," in *Proceedings of 7th Congress of the ISRM*, pp. 333–340, Aachen, Germany, 1991.

[14] M. Sagong and A. Bobet, "Coalescence of multiple flaws in a rock-model material in uniaxial compression," *International Journal of Rock Mechanics and Mining Sciences*, vol. 39, no. 2, pp. 229–241, 2002.

[15] L. N. Y. Wong and H. H. Einstein, "Crack coalescence in molded gypsum and carrara marble: Part 1. Macroscopic observations and interpretation," *Rock Mechanics and Rock Engineering*, vol. 42, no. 3, pp. 475–511, 2008.

[16] L. N. Y. Wong and H. H. Einstein, "Crack coalescence in molded gypsum and carrara marble: Part 2-microscopic observations and interpretation," *Rock Mechanics and Rock Engineering*, vol. 42, no. 3, pp. 513–545, 2008.

[17] H. Lee and S. Jeon, "An experimental and numerical study of fracture coalescence in pre-cracked specimens under uniaxial compression," *International Journal of Solids and Structures*, vol. 48, no. 6, pp. 979–999, 2011.

[18] S.-Q. Yang, "Crack coalescence behavior of brittle sandstone samples containing two coplanar fissures in the process of deformation failure," *Engineering Fracture Mechanics*, vol. 78, pp. 3059–3081, 2011.

[19] P. Cao, T. Liu, C. Pu, and H. Lin, "Crack propagation and coalescence of brittle rock-like specimens with pre-existing cracks in compression," *Engineering Geology*, vol. 187, no. 17, pp. 113–121, 2015.

[20] R.-h. Cao, P. Cao, X. Fan, X. Xiong, and H. Lin, "An experimental and numerical study on mechanical behavior of ubiquitous-joint brittle rock-like specimens under uniaxial compression," *Rock Mechanics and Rock Engineering*, vol. 49, pp. 4319–4338, 2016.

[21] K. Zhang, P. Cao, G. Ma, W. Wang, W. Fan, and K. Li, "Strength, fragmentation and fractal properties of mixed flaws," *Acta Geotechnica*, vol. 11, pp. 901–912, 2015.

[22] R. H. C. Wong and K. T. Chau, "Crack coalescence in a rock-like material containing two cracks," *International Journal of Rock Mechanics and Mining Sciences*, vol. 35, no. 2, pp. 147–164, 1998.

[23] C. H. Park and A. Bobet, "Crack coalescence in specimens with open and closed flaws: a comparison," *International Journal of Rock Mechanics and Mining Sciences*, vol. 46, no. 5, pp. 819–829, 2009.

[24] P. H. S. W. Kulatilake, B. Malama, and J. Wang, "Physical and particle flow modeling of jointed rock block behavior under uniaxial loading," *International Journal of Rock Mechanics and Mining Sciences*, vol. 38, pp. 641–657, 2001.

[25] S. P. Morgan, C. A. Johnson, and H. H. Einstein, "Cracking processes in Barre granite: fracture process zones and crack coalescence," *International Journal of Fracture*, vol. 180, pp. 177–204, 2013.

[26] Q. Yin, H. W. Jing, and T. T. Zhu, "Mechanical behavior and failure analysis of granite specimens containing two orthogonal fissures under uniaxial compression," *Arabian Journal of Geosciences*, vol. 9, no. 31, 2016.

[27] P. Yin, R. H. C. Wong, and K. T. Chau, "Coalescence of two parallel pre-existing surface cracks in granite," *International Journal of Rock Mechanics and Mining Sciences*, vol. 68, pp. 66–84, 2014.

[28] S.-Q. Yang and H.-W. Jing, "Strength failure and crack coalescence behavior of brittle sandstone samples containing a single fissure under uniaxial compression," *International Journal of Fracture*, vol. 168, pp. 227–250, 2010.

[29] S. Q. Yang, D. S. Yang, H. W. Jing, Y. H. Li, and S. Y. Wang, "An experimental study of the fracture coalescence behaviour of brittle sandstone specimens containing three fissures," *Rock Mechanics and Rock Engineering*, vol. 45, no. 4, pp. 563–582, 2011.

[30] S.-Q. Yang, W.-L. Tian, Y.-H. Huang, P. G. Ranjith, and Y. Ju, "An experimental and numerical study on cracking behavior of brittle sandstone containing two non-coplanar fissures under uniaxial compression," *Rock Mechanics and Rock Engineering*, vol. 49, no. 4, pp. 1497–1515, 2015.

[31] S.-Q. Yang, Y.-H. Huang, W.-L. Tian, and J.-B. Zhu, "An experimental investigation on strength, deformation and crack evolution behavior of sandstone containing two oval flaws under uniaxial compression," *Engineering Geology*, vol. 217, pp. 35–48, 2017.

[32] J.-P. Petit and M. Barquins, "Can natural faults propagate under mode II conditions?," *Tectonics*, vol. 7, no. 6, pp. 1243–1256, 2010.

[33] Y. Lu, L. Wang, and D. Elsworth, "Uniaxial strength and failure in sandstone containing a pre-existing 3-D surface flaw," *International Journal of Fracture*, vol. 194, pp. 59–79, 2015.

[34] Y. X. Wang, H. Lin, Y. L. Zhao, X. Li, P. P. Guo, and Y. Liu, "Analysis of fracturing characteristics of unconfined rock plate under edge on impact loading," *European Journal of Environmental and Civil Engineering*, 2019.

[35] M.-D. Wei, F. Dai, N.-W. Xu, Y. Liu, and T. Zhao, "A novel chevron notched short rod bend method for measuring the mode I fracture toughness of rocks," *Engineering Fracture Mechanics*, vol. 190, pp. 1–15, 2018.

[36] M.-D. Wei, F. Dai, N.-W. Xu, T. Zhao, and Y. Liu, "An experimental and theoretical assessment of semi-circular bend specimens with chevron and straight-through notches for mode I fracture toughness testing of rocks," *International Journal of Rock Mechanics and Mining Sciences*, vol. 99, pp. 28–38, 2017.

[37] M. D. Wei, F. Dai, N. W. Xu, and T. Zhao, "Experimental and numerical investigation of cracked chevron notched Brazilian disc specimen for fracture toughness testing of rock," *Fatigue & Fracture of Engineering Materials & Structures*, vol. 41, pp. 197–211, 2017.

[38] X. Fan, R. Chen, H. Lin, H. Lai, C. Zhang, and Q. Zhao, "Cracking and failure in rock specimen containing combined flaw and hole under uniaxial compression," *Advances in Civil Engineering*, vol. 2018, pp. 1–15, 2018.

[39] D. Huang, D. Gu, C. Yang, R. Huang, and G. Fu, "Investigation on mechanical behaviors of sandstone with two preexisting flaws under triaxial compression," *Rock Mechanics and Rock Engineering*, vol. 49, pp. 375–399, 2015.

[40] Y.-P. Li, L.-Z. Chen, and Y.-H. Wang, "Experimental research on pre-cracked marble under compression," *International Journal of Solids and Structures*, vol. 42, no. 9/10, pp. 2505–2516, 2005.

[41] Z. Brooks, F.-J. Ulm, and H. H. Einstein, "Environmental scanning electron microscopy (ESEM) and nanoindentation investigation of the crack tip process zone in marble," *Acta Geotechnica*, vol. 8, pp. 223–245, 2013.

[42] S. Q. Yang, Y. H. Dai, L. J. Han, and Z. Q. Jin, "Experimental study on mechanical behavior of brittle marble samples containing different flaws under uniaxial compression," *Engineering Fracture Mechanics*, vol. 76, pp. 1833–1845, 2009.

[43] L. N. Y. Wong and H. H. Einstein, "Systematic evaluation of cracking behavior in specimens containing single flaws under uniaxial compression," *International Journal of Rock Mechanics and Mining Sciences*, vol. 46, pp. 239–249, 2009.

[44] Y. Cheng, L. N. Y. Wong, and C. Zou, "Experimental study on the formation of faults from en-echelon fractures in Carrara Marble," *Engineering Geology*, vol. 195, pp. 312–326, 2015.

[45] G. Chen, J. M. Kemeny, and S. Harpalani, "Fracture propagation and coalescence in marble plates with pre-cut notches under compression," in *Proceedings of the Symposium on Fractured, Jointed Rock Masses*, Lake Tahoe, CA, USA, 1995.

[46] R. H. C. Wong, C. M. Law, K. T. Chau, and W.-S. Zhu, "Crack propagation from 3-D surface fractures in PMMA and marble specimens under uniaxial compression," *International Journal of Rock Mechanics and Mining Sciences*, vol. 41, no. 3, pp. 360–366, 2004.

[47] A. M. Ferrero and P. Marini, "Experimental studies on the mechanical behaviour of two thermal cracked marbles," *Rock Mechanics and Rock Engineering*, vol. 34, no. 1, pp. 57–66, 2001.

[48] G. S. Xeidakis, I. S. Samaras, D. A. Zacharopoulos, and G. E. Papakaliatakis, "Trajectories of unstably growing cracks in mixed mode I-II loading of marble beams," *Rock Mechanics and Rock Engineering*, vol. 30, no. 1, pp. 19–33, 1997.

[49] M. Migliazza, A. M. Ferrero, and A. Spagnoli, "Experimental investigation on crack propagation in Carrara marble subjected to cyclic loads," *International Journal of Rock Mechanics and Mining Sciences*, vol. 48, pp. 1038–1044, 2011.

[50] S. P. Morgan and H. H. Einstein, "Cracking processes affected by bedding planes in Opalinus shale with flaw pairs," *Engineering Fracture Mechanics*, vol. 176, pp. 213–234, 2017.

[51] A. R. Ingraffea and F. E. Heuze, "Finite element models for rock fracture mechanics," *International Journal for Numerical and Analytical Methods in Geomechanics*, vol. 4, no. 1, pp. 25–43, 1980.

[52] M. Prudencio and M. Van Sint Jan, "Strength and failure modes of rock mass models with non-persistent joints," *International Journal of Rock Mechanics and Mining Sciences*, vol. 44, pp. 890–902, 2007.

[53] R.-h. Cao, P. Cao, H. Lin, C.-z. Pu, and K. Ou, "Mechanical behavior of brittle rock-like specimens with pre-existing fissures under uniaxial loading: experimental studies and particle mechanics approach," *Rock Mechanics and Rock Engineering*, vol. 49, no. 3, pp. 763–783, 2015.

[54] R.-h. Cao, P. Cao, H. Lin, G. Ma, and Y. Chen, "Failure characteristics of intermittent fissures under a compressive-shear test: experimental and numerical analyses," *Theoretical and Applied Fracture Mechanics*, vol. 96, pp. 740–757, 2018.

[55] Y. Liu and F. Dai, "A damage constitutive model for intermittent jointed rocks under cyclic uniaxial compression," *International Journal of Rock Mechanics and Mining Sciences*, vol. 103, pp. 289–301, 2018.

[56] P. Feng, F. Dai, Y. Liu, N. Xu, and T. Zhao, "Effects of strain rate on the mechanical and fracturing behaviors of rock-like specimens containing two unparallel fissures under uniaxial compression," *Soil Dynamics and Earthquake Engineering*, vol. 110, pp. 195–211, 2018.

[57] P. Feng, F. Dai, Y. Liu, N. Xu, and P. Fan, "Effects of coupled static and dynamic strain rates on mechanical behaviors of rock-like specimens containing pre-existing fissures under uniaxial compression," *Canadian Geotechnical Journal*, vol. 55, pp. 640–652, 2018.

[58] Y. Zhao, L. Zhang, W. Wang, C. Pu, W. Wan, and J. Tang, "Cracking and stress-strain behavior of rock-like material containing two flaws under uniaxial compression," *Rock Mechanics and Rock Engineering*, vol. 49, pp. 2665–2687, 2016.

[59] J. Jin, P. Cao, Y. Chen, C. Pu, D. Mao, and X. Fan, "Influence of single flaw on the failure process and energy mechanics of rock-like material," *Computers and Geotechnics*, vol. 86, pp. 150–162, 2017.

[60] O. Mughieda, A. K. Alzo'ubi, and Alzoubi, "Fracture mechanisms of offset rock joints-A laboratory investigation," *Geotechnical and Geological Engineering*, vol. 22, pp. 545–562, 2004.

[61] O. Mughieda and I. Karasneh, "Coalescence of offset rock joints under biaxial loading," *Geotechnical and Geological Engineering*, vol. 24, pp. 985–999, 2006.

[62] H. Haeri, K. Shahriar, M. F. Marji, and P. Moarefvand, "Experimental and numerical study of crack propagation and coalescence in pre-cracked rock-like disks," *International Journal of Rock Mechanics and Mining Sciences*, vol. 67, pp. 20–28, 2014.

[63] Y. Liu, F. Dai, P. Fan, N. Xu, and L. Dong, "Experimental investigation of the influence of joint geometric configurations on the mechanical properties of intermittent jointed rock models under cyclic uniaxial compression," *Rock Mechanics and Rock Engineering*, vol. 50, pp. 1453–1471, 2017.

[64] Y.-H. Huang, S.-Q. Yang, W.-L. Tian, W. Zeng, and L.-Y. Yu, "An experimental study on fracture mechanical behavior of rock-like materials containing two unparallel fissures under uniaxial compression," *Acta Mechanica Sinica*, vol. 32, pp. 442–455, 2015.

[65] H. W. Jing, S. Q. Yang, M. L. Zhang, G. A. Xu, and K. F. Chen, "An experimental study on anchorage strength and deformation behavior of large-scale jointed rock mass," *Tunnelling and Underground Space Technology*, vol. 43, pp. 184–197, 2014.

[66] T. Liu, B. Lin, and W. Yang, "Mechanical behavior and failure mechanism of pre-cracked specimen under uniaxial compression," *Tectonophysics*, vol. 712-713, pp. 330–343, 2017.

[67] V. Sarfarazi, A. Ghazvinian, W. Schubert, M. Blumel, and H. R. Nejati, "Numerical simulation of the process of fracture of echelon rock joints," *Rock Mechanics and Rock Engineering*, vol. 47, pp. 1355–1371, 2013.

[68] A. Ghazvinian, V. Sarfarazi, and W. Schubert, "A study of the failure mechanism of planar non-persistent open joints using PFC2D," *Rock Mechanics and Rock Engineering*, vol. 45, pp. 677–693, 2012.

[69] X.-P. Zhang, Q. Liu, S. Wu, and X. Tang, "Crack coalescence between two non-parallel flaws in rock-like material under uniaxial compression," *Engineering Geology*, vol. 199, pp. 74–90, 2015.

[70] P. L. P. Wasantha, P. G. Ranjith, D. R. Viete, and L. Luo, "Influence of the geometry of partially-spanning joints on the uniaxial compressive strength of rock," *International Journal of Rock Mechanics and Mining Sciences*, vol. 50, pp. 140–146, 2012.

[71] R. H. Cao, P. Cao, H. Lin, G. W. Ma, X. Fan, and X. G. Xiong, "Mechanical behavior of an opening in a jointed rock-like specimen under uniaxial loading: experimental studies and particle mechanics approach," *Archives of civil and mechanical engineering*, vol. 18, pp. 198–214, 2018.

[72] R. H. Cao, P. Cao, H. Lin, G. W. Ma, C. Y. Zhang, and C. Jiang, "Failure characteristics of jointed rock-like material containing multi-joints under a compressive-shear test: experimental and numerical analyses," *Archives of Civil and Mechanical Engineering*, vol. 18, pp. 784–798, 2018.

[73] R. Cao, P. Cao, H. Lin, and X. Fan, "Experimental and numerical study of the failure process and energy mechanisms of rock-like materials containing cross un-persistent joints under uniaxial compression," *PLOS One*, vol. 12, Article ID e0188646, 2017.

[74] R.-h. Cao and H. Lin, "Experimental and numerical study of failure behavior and energy mechanics of rock-like materials containing multiple joints," *Advances in Materials Science and Engineering*, vol. 2017, Article ID 6460150, 17 pages, 2017.

[75] Q. B. Lin, P. Cao, K. H. Li, R. H. Cao, K. P. Zhou, and H. W. Deng, "Experimental study on acoustic emission characteristics of jointed rock mass under two TBM disc cutters," *Journal of Central South University*, vol. 25, no. 2, pp. 357–367, 2017.

[76] Q. Lin, P. Cao, and R. Cao, "Experimental investigation of jointed rock breaking under a disc cutter with different confining stresses," *Comptes Rendus Mécanique*, vol. 346, pp. 833–843, 2018.

[77] A. Bobet, "Fracture coalescence in rock materials: experimental observations and numerical predictions," Sc.D. Thesis, MIT, Cambridge, USA, 1997.

[78] M. Sagong and A. Bobet, "Coalescence of multiple flaws in uniaxial compression," in *Proceedings of the North American Rock Mechanics Symposium: Pacific Rocks*, pp. 1203–1210, 2000.

[79] Q. Liu, J. Xu, X. Liu, J. Jiang, and B. Liu, "The role of flaws on crack growth in rock-like material assessed by AE technique," *International Journal of Fracture*, vol. 193, pp. 99–115, 2015.

[80] X.-X. Yang, H.-W. Jing, C.-A. Tang, and S.-Q. Yang, "Effect of parallel joint interaction on mechanical behavior of jointed rock mass models," *International Journal of Rock Mechanics and Mining Sciences*, vol. 92, pp. 40–53, 2017.

[81] H. Cheng, X. Zhou, J. Zhu, and Q. Qian, "The effects of crack openings on crack initiation, propagation and coalescence behavior in rock-like materials under uniaxial compression," *Rock Mechanics and Rock Engineering*, vol. 49, pp. 3481–3494, 2016.

[82] X. P. Zhou, H. Cheng, and Y. F. Feng, "An experimental study of crack coalescence behaviour in rock-like materials containing multiple flaws under uniaxial compression," *Rock Mechanics and Rock Engineering*, vol. 47, pp. 1961–1986, 2013.

[83] C. Gehle and H. K. Kutter, "Breakage and shear behaviour of intermittent rock joints," *International Journal of Rock Mechanics and Mining Sciences*, vol. 40, pp. 687–700, 2003.

[84] E. Gerolymatou and T. Triantafyllidis, "Shearing of materials with intermittent joints," *Rock Mechanics and Rock Engineering*, vol. 49, pp. 2689–2700, 2016.

[85] C. H. Park and A. Bobet, "Crack initiation, propagation and coalescence from frictional flaws in uniaxial compression," *Engineering Fracture Mechanics*, vol. 77, no. 14, pp. 2727–2748, 2010.

[86] R. H. C. Wong, P. Lin, C. A. Tang, and K. T. Chau, "Creeping damage around an opening in rock-like material containing non-persistent joints," *Engineering Fracture Mechanics*, vol. 69, pp. 2015–2027, 2002.

[87] H. H. Einstein and F. S. Jeng, "Model experiments for propellant embedded rock anchors," *Rock Mechanics and Rock Engineering*, vol. 24, pp. 1–29, 1991.

[88] X. Chen, Z. Liao, and X. Peng, "Deformability characteristics of jointed rock masses under uniaxial compression," *International Journal of Mining Science and Technology*, vol. 22, pp. 213–221, 2012.

[89] M. L. Huang and R. H. C. Wong, "Experimental study on propagation and coalescence mechanisms of 3D surface cracks," *Chinese Journal of Rock Mechanics and Engineering*, vol. 26, pp. 1794–1799, 2007.

[90] M. L. Huang and R. H. C. Wong, "Experimental study on propagation and coalescence mechanisms of 3D surface cracks," *Chinese Journal of Rock Mechanics and Engineering*, vol. 21, no. 6, pp. 1794–1798, 2007, in Chinese.

[91] N. P. Cannon, E. M. Schulson, T. R. Smith, and H. J. Frost, "Wing cracks and brittle compressive fracture," *Acta Metallurgica et Materialia*, vol. 38, no. 10, pp. 1955–1962, 1990.

[92] A. V. Dyskin, E. Sahouryeh, R. J. Jewell, H. Joer, and K. B. Ustinov, "Influence of shape and locations of initial 3-D cracks on their growth in uniaxial compression," *Engineering Fracture Mechanics*, vol. 70, no. 15, pp. 2115–2136, 2003.

[93] E. Sahouryeh, A. V. Dyskin, and L. N. Germanovich, "Crack growth under biaxial compression," *Engineering Fracture Mechanics*, vol. 69, no. 18, pp. 2187–2198, 2002.

[94] Y. S. Guo, C. J. Lin, W. S. Zhu, and S. C. Li, "Experimental research on propagation and coalescence process of three-dimensional flaw-sets," *Chinese Journal of Rock Mechanics and Engineering*, vol. 27, no. 9, pp. 3191–3195, 2008, in Chinese.

[95] H. D. Tang, Z. D. Zhu, M. L. Zhu, and H. X. Lin, "Mechanical behavior of 3D crack growth in transparent rock-like material containing preexisting flaws under compression," *Advances in Materials Science and Engineering*, vol. 2015, Article ID 193721, 10 pages, 2015.

[96] Y. Ju, L. Wang, H. Xie, G. Ma, Z. Zheng, and L. Mao, "Visualization and transparentization of the structure and stress field of aggregated geomaterials through 3D printing and photoelastic techniques," *Rock Mechanics and Rock Engineering*, vol. 50, pp. 1383–1407, 2017.

[97] A. V. Dyskin, L. N. Germanovich, R. J. Jewell et al., "Study of 3-d mechanisms of crack growth and interaction in uniaxial compression," *ISRM News Journal*, vol. 2, no. 1, pp. 17–24, 1994.

[98] J.-W. Fu, K. Chen, W.-s. Zhu, X.-z. Zhang, and X.-j. Li, "Progressive failure of new modelling material with a single internal crack under biaxial compression and the 3-D numerical simulation," *Engineering Fracture Mechanics*, vol. 165, pp. 140–152, 2016.

[99] Z. T. Bieniawski, "Mechanism of brittle fracture of rock," *International Journal of Rock Mechanics and Mining Sciences & Geomechanics Abstracts*, vol. 4, pp. 407–423, 1967.

[100] W. F. Brace and E. G. Bombolakis, "A note on brittle crack growth in compression," *Journal of Geophysical Research*, vol. 68, no. 12, pp. 3709–3713, 2012.

[101] N. Y. Wong, *Crack Coalescence in Molded Gypsum and Carrara Marble (Ph.D.)*, Massachusetts Institute of Technology, Cambridge, MA, USA, 2008.

[102] R. L. Kranz, "Crack-crack and crack-pore interactions in stressed granite," *International Journal of Rock Mechanics and Mining Sciences & Geomechanics Abstracts*, vol. 16, pp. 37–47, 1979.

[103] M. L. Batzle, G. Simmons, and R. W. Siegfried, "Microcrack closure in rocks under stress: direct observation," *Journal of Geophysical Research*, vol. 85, pp. 7072–7090, 1980.

[104] L. N. Germanovich, B. J. Carter, A. V. Dyskin, A. R. Ingraffea, and K. K. Lee, "Mechanics of 3-D crack growth under compressive loads. Rock mechanics tools and techniques," in *Proceedings of the Second North American Rock Mechanics Symposium: NARMS '96*, pp. 1151–1160, Balkema, Rotterdam, Netherlands, 1996.

[105] P. S. Steif, "Crack extension under compressive loading," *Engineering Fracture Mechanics*, vol. 20, no. 3, pp. 463–473, 1984.

[106] L. E. Vallejo, "The influence of fissures in a stiff clay subjected to direct shear," *Géotechnique*, vol. 37, no. 1, pp. 69–82, 1987.

[107] L. N. Y. Wong and H.-Q. Li, "Numerical study on coalescence of two pre-existing coplanar flaws in rock," *International Journal of Solids and Structures*, vol. 50, no. 22-23, pp. 3685–3706, 2013.

[108] C. A. Tang, P. Lin, R. H. C. Wong, and K. T. Chau, "Analysis of crack coalescence in rock-like materials containing three flaws-Part II: numerical approach," *International Journal of Rock Mechanics and Mining Sciences*, vol. 38, no. 7, pp. 925–939, 2001.

[109] B. Vásárhelyi and A. Bobet, "Modeling of crack initiation, propagation and coalescence in uniaxial compression," *Rock Mechanics and Rock Engineering*, vol. 33, no. 2, pp. 119–139, 2000.

[110] R. H. C. Wong, W. L. Leung, and S. W. Wang, "Shear strength study on rock-like models containing arrayed open joints," in *Rock Mechanics in the National Interest*, pp. 843–849, Swets & Zeitlinger Lisse, The Netherland, 2001.

[111] X.-P. Zhang and L. N. Y. Wong, "Crack initiation, propagation and coalescence in rock-like material containing two flaws: a numerical study based on bonded-particle model approach," *Rock Mechanics and Rock Engineering*, vol. 46, pp. 1001–1021, 2012.

[112] X.-P. Zhang and L. N. Y. Wong, "Loading rate effects on cracking behavior of flaw-contained specimens under uniaxial compression," *International Journal of Fracture*, vol. 180, pp. 93–110, 2013.

[113] S.-Q. Yang, X.-R. Liu, and H.-W. Jing, "Experimental investigation on fracture coalescence behavior of red sandstone containing two unparallel fissures under uniaxial compression," *International Journal of Rock Mechanics and Mining Sciences*, vol. 63, pp. 82–92, 2013.

[114] W. W. Chen and B. Song, *Split Hopkinson (Kolsky) Bar: Design, Testing And Applications*, Springer, New York, NY, USA, 2011.

[115] Y.-H. Huang, S.-Q. Yang, and J. Zhao, "Three-Dimensional numerical simulation on triaxial failure mechanical behavior of rock-like specimen containing two unparallel fissures," *Rock Mechanics and Rock Engineering*, vol. 49, pp. 4711–4729, 2016.

[116] J. Chen and X. Feng, "True triaxial experimental study on rock with high geostress," *Chinese Journal of Rock Mechanics and Engineering*, vol. 25, no. 8, pp. 1537–1543, 2006.

[117] X. Li, K. Du, and D. Li, "True triaxial strength and failure modes of cubic rock specimens with unloading the minor principal stress," *Rock Mechanics and Rock Engineering*, vol. 48, pp. 2185–2196, 2015.

[118] ISRM, "Suggested methods for determining tensile strength of rock materials," *International Journal of Rock Mechanics and Mining Sciences*, vol. 15, no. 3, pp. 99–103, 1978.

[119] ASTM, *D2936-08 Standard Test Method for Direct Tensile Strength of Intact Rock Core Specimens*, Annual book of ASTM standards. ASTM International, West Conshohocken, PA, USA, 2008.

[120] ASTM, *D3967-08 Standard Test Method for Splitting Tensile Strength of Intact Rock Core Specimens*, Annual book of ASTM standards. ASTM International, West Conshohocken, PA, USA, 2008.

[121] G. Khanlari, B. Rafiei, and Y. Abdilor, "An experimental investigation of the Brazilian tensile strength and failure patterns of laminated sandstones," *Rock Mechanics and Rock Engineering*, vol. 48, pp. 843–852, 2014.

[122] Y.-W. Li, J. Zhang, and Y. Liu, "Effects of loading direction on failure load test results for Brazilian tests on coal rock," *Rock Mechanics and Rock Engineering*, vol. 49, pp. 2173–2180, 2015.

[123] L. Yang, Y. Jiang, S. Li, and B. Li, "Experimental and numerical research on 3D crack growth in rocklike material subjected to uniaxial tension," *Journal of Geotechnical and Geoenvironmental Engineering*, vol. 139, no. 10, pp. 1781–1788, 2013.

[124] E. Z. Lajtai, "Strength of discontinuous rocks in direct shear," *Géotechnique*, vol. 19, pp. 218–233, 1969.

[125] E. Z. Lajtai, "Shear strength of weakness planes in rock," *International Journal of Rock Mechanics and Mining Sciences & Geomechanics Abstracts*, vol. 6, pp. 499–515, 1969.

[126] T. Savilahti, E. Nordlund, and O. Stephansson, "Shear box testing and modeling of joint bridge," in *Proceedings of International Symposium on Shear Box Testing and Modeling of Joint Bridge Rock Joints*, pp. 295–300, Norway, 1990.

[127] H. Wang and H. Lin H, "Non-linear shear strength criterion for a rock joint with consideration of friction variation," *Geotechnical and Geological Engineering*, vol. 36, no. 6, pp. 3731–3741, 2018.

[128] H. Lin, M. Wang, and W. Xu, "Shear behaviors of the binary structural plane," *Geotechnical and Geological Engineering*, vol. 36, pp. 939–948, 2018.

[129] A. Ghazvinian, M. R. Nikudel, and V. Sarfarazi, "Effect of rock bridge continuity and area on shear behavior of joints," in *Proceedings of the 11th Congress of the International Society for Rock Mechanics*, Lisbon, Portugal, 2007.

[130] D. Huang, D. Cen, G. Ma, and R. Huang, "Step-path failure of rock slopes with intermittent joints," *Landslides*, vol. 12, pp. 911–926, 2014.

[131] N. T. Burdine, "Rock failure under dynamic loading conditions," *Society of Petroleum Engineers Journal*, vol. 3, pp. 1–8, 2013.

[132] P. B. Attewell and I. W. Farmer, "Fatigue behaviour of rock," *International Journal of Rock Mechanics and Mining Sciences & Geomechanics Abstracts*, vol. 10, pp. 1–9, 1973.

[133] Z. Y. Tao and H. H. Mo, "An experimental study and analysis of the behaviour of rock under cyclic loading," *International Journal of Rock Mechanics and Mining Sciences & Geomechanics Abstracts*, vol. 27, no. 1, pp. 51–56, 1990.

[134] S. K. Ray, M. Sarkar, and T. N. Singh, "Effect of cyclic loading and strain rate on the mechanical behaviour of sandstone," *International Journal of Rock Mechanics and Mining Sciences*, vol. 36, no. 4, pp. 543–549, 1999.

[135] M. N. Bagde and V. Petroš, "Fatigue properties of intact sandstone samples subjected to dynamic uniaxial cyclical loading," *International Journal of Rock Mechanics and Mining Sciences*, vol. 42, no. 2, pp. 237–250, 2005a.

[136] M. N. Bagde and V. Petroš, "Waveform effect on fatigue properties of intact sandstone in uniaxial cyclical loading," *Rock Mechanics and Rock Engineering*, vol. 38, no. 3, pp. 169–196, 2005.

[137] K. Fuenkajorn and D. Phueakphum, "Effects of cyclic loading on mechanical properties of Maha Sarakham salt," *Engineering Geology*, vol. 112, pp. 43–52, 2010.

[138] L.-j. Ma, X.-y. Liu, M.-y. Wang et al., "Experimental investigation of the mechanical properties of rock salt under triaxial cyclic loading," *International Journal of Rock Mechanics and Mining Sciences*, vol. 62, pp. 34–41, 2013.

[139] Y. Xu, F. Dai, T. Zhao, N.-w. Xu, and Y. Liu, "Fracture toughness determination of cracked chevron notched Brazilian disc rock specimen via Griffith energy criterion incorporating realistic fracture profiles," *Rock Mechanics and Rock Engineering*, vol. 49, pp. 3083–3093, 2016.

[140] E. T. Brown and J. A. Hudson, "Fatigue failure characteristics of some models of jointed rock," *Earthquake Engineering & Structural Dynamics*, vol. 2, pp. 379–386, 1974.

[141] G. L. Prost, "Jointing at rock contacts in cyclic loading," *International Journal of Rock Mechanics and Mining Sciences & Geomechanics Abstracts*, vol. 25, no. 5, pp. 263–272, 1988.

[142] N. Li, W. Chen, P. Zhang, and G. Swoboda, "The mechanical properties and a fatigue-damage model for jointed rock masses subjected to dynamic cyclical loading," *International Journal of Rock Mechanics and Mining Sciences*, vol. 38, pp. 1071–1079, 2001.

[143] N. Erarslan and D. J. Williams, "Experimental, numerical and analytical studies on tensile strength of rocks," *International Journal of Rock Mechanics and Mining Sciences*, vol. 49, pp. 21–30, 2012.

[144] H. Lin, W. Xiong, and Q. Yan, "Three-dimensional effect of tensile strength in the standard Brazilian test considering contact length," *Geotechnical Testing Journal*, vol. 39, no. 1, pp. 137–143, 2016.

[145] C. A. Tang and S. Q. Kou, "Crack propagation and coalescence in brittle materials under compression," *Engineering Fracture Mechanics*, vol. 61, pp. 311–324, 1998.

[146] N. Moës, J. Dolbow, and T. Belytschko, "A finite element method for crack growth without remeshing," *International Journal for Numerical Methods in Engineering*, vol. 46, pp. 131–150, 1999.

[147] N. Moës and T. Belytschko, "Extended finite element method for cohesive crack growth," *Engineering Fracture Mechanics*, vol. 69, pp. 813–833, 2002.

[148] P. Areias and T. Rabczuk, "Finite strain fracture of plates and shells with configurational forces and edge rotations," *International Journal for Numerical Methods in Engineering*, vol. 94, pp. 1099–1122, 2013.

[149] P. Areias, D. Dias-da-Costa, J. Alfaiate, and E. Júlio, "Arbitrary bi-dimensional finite strain cohesive crack propagation," *Computational Mechanics*, vol. 45, no. 1, pp. 61–75, 2009.

[150] T. N. Bittencourt, P. A. Wawrzynek, A. R. Ingraffea, and J. L. Sousa, "Quasi-automatic simulation of crack propagation for 2D LEFM problems," *Engineering Fracture Mechanics*, vol. 55, no. 2, pp. 321–334, 1996.

[151] D. Colombo and M. Giglio, "A methodology for automatic crack propagation modelling in planar and shell FE models," *Engineering Fracture Mechanics*, vol. 73, pp. 490–504, 2006.

[152] G.-H. Shi and R. E. Goodman, "Generalization of two-dimensional discontinuous deformation analysis for forward modelling," *International Journal for Numerical and Analytical Methods in Geomechanics*, vol. 13, pp. 359–380, 1989.

[153] J. Gu and Z. Zhao, "Considerations of the discontinuous deformation analysis on wave propagation problems," *International Journal for Numerical and Analytical Methods in Geomechanics*, vol. 33, no. 12, pp. 1449–1465, 2009.

[154] Y. J. Ning, J. Yang, X. M. An, and G. W. Ma, "Modelling rock fracturing and blast induced rock mass failure via advanced discretization within the discontinuous deformation analysis framework," *Computers and Geotechnics*, vol. 38, no. 1, pp. 40–49, 2010.

[155] Y. J. Ning, X. M. An, and G. W. Ma, "Footwall slope stability analysis with the numerical manifold method," *International Journal of Rock Mechanics and Mining Sciences*, vol. 48, pp. 964–975, 2011.

[156] G. H. Shi, "Manifold method of material analysis," in *Transactions of the 9th Army Conference on Applied Mathematics and Computing*, pp. 57–76, Minneapolis, MN, USA, 1992.

[157] G. W. Ma, X. M. An, H. H. Zhang, and L. X. Li, "Modeling complex crack problems using the numerical manifold method," *International Journal of Fracture*, vol. 156, no. 1, pp. 21–35, 2009.

[158] H. H. Zhang, L. X. Li, X. M. An, and G. W. Ma, "Numerical analysis of 2-D crack propagation problems using the numerical manifold method," *Engineering Analysis with Boundary Elements*, vol. 34, no. 1, pp. 41–50, 2010.

[159] L. B. Lucy, "A numerical approach to the testing of the fission hypothesis," *Astronomical Journal*, vol. 82, no. 12, pp. 1013–1024, 1977.

[160] R. A. Gingold and J. J. Monaghan, "Smoothed particle hydrodynamics: theory and application to non-spherical stars," *Monthly Notices of the Royal Astronomical Society*, vol. 181, pp. 375–389, 1977.

[161] R. Pramanik and D. Deb, "SPH procedures for modeling multiple intersecting discontinuities in geomaterial," *International Journal for Numerical and Analytical Methods in Geomechanics*, vol. 39, no. 4, pp. 343–367, 2014.

[162] V. Mehra and S. Chaturvedi, "High velocity impact of metal sphere on thin metallic plates: a comparative smooth particle hydrodynamics study," *Journal of Computational Physics*, vol. 212, pp. 318–337, 2006.

[163] H. Lin, H. Wang, X. Fan, P. Cao, and K. Zhou, "Particle size distribution effects on deformation properties of graded aggregate base under cyclic loading," *European Journal of Environmental and Civil Engineering*, vol. 40, pp. 1–18, 2018.

[164] R. Cao, W. Tang, H. Lin, and X. Fan, "Numerical analysis for the progressive failure of binary-medium interface under shearing," *Advances in Civil Engineering*, vol. 41, pp. 71-72, 2018.

[165] C. Zhang, C. Qiu, C. Pu, X. Fan, and P. Cao, "The mechanism of vibrations-aided gravitational flow with overhanging style in hopper," *Powder Technology*, vol. 327, pp. 291–302, 2018.

[166] A. Manouchehrian and M. F. Marji, "Numerical analysis of confinement effect on crack propagation mechanism from a flaw in a pre-cracked rock under compression," *Acta Mechanica Sinica*, vol. 28, no. 5, pp. 1389–1397, 2012.

[167] X. Fan, K. Li, H. Lai, Y. Xie, R. Cao, and J. Zheng, "Internal stress distribution and cracking around flaws and openings of rock block under uniaxial compression: a particle mechanics approach," *Computers and Geotechnics*, vol. 102, pp. 28–38, 2018.

[168] M. Bahaaddini, G. Sharrock, and B. K. Hebblewhite, "Numerical investigation of the effect of joint geometrical parameters on the mechanical properties of a non-persistent jointed rock mass under uniaxial compression," *Computers and Geotechnics*, vol. 49, pp. 206–225, 2013.

[169] X. Fan, H. Lin, H. P. Lai, R. H. Cao, and J. Liu, "Numerical analysis for the compressive and shear failure behaviors of rock containing multi-intermittent joints," *Comptes Rendus Mecanique*, vol. 347, pp. 1315–1325, 2019.

[170] K. Li, Y. Cheng, and X. Fan, "Roles of model size and particle size distribution on macro-mechanical properties of Lac du Bonnet granite using flat-joint model," *Computers and Geotechnics*, vol. 103, pp. 43–60, 2018.

[171] X.-P. Zhang and L. N. Y. Wong, "Displacement field analysis for cracking processes in bonded-particle model," *Bulletin of Engineering Geology and the Environment*, vol. 73, pp. 13–21, 2013.

[172] X. Fan, P. H. S. W. Kulatilake, and X. Chen, "Mechanical behavior of rock-like jointed blocks with multi-non-persistent joints under uniaxial loading: a particle mechanics approach," *Engineering Geology*, vol. 190, no. 14, pp. 17–32, 2015.

[173] H. Li and L. N. Y. Wong, "Influence of flaw inclination angle and loading condition on crack initiation and propagation," *International Journal of Solids and Structures*, vol. 49, pp. 2482–2499, 2012.

[174] Y. Xie, P. Cao, J. Liu, and L. Dong, "Influence of crack surface friction on crack initiation and propagation: a numerical investigation based on extended finite element method," *Computers and Geotechnics*, vol. 74, pp. 1–14, 2016.

[175] R. H. C. Wong, C. A. Tang, K. T. Chau, and P. Lin, "Splitting failure in brittle rocks containing pre-existing flaws under uniaxial compression," *Engineering Fracture Mechanics*, vol. 69, pp. 1853–1871, 2002.

[176] H. Q. Zhang, Z. Y. Zhao, C. A. Tang, and L. Song, "Numerical study of shear behavior of intermittent rock joints with different geometrical parameters," *International Journal of Rock Mechanics and Mining Sciences*, vol. 43, pp. 802–816, 2006.

[177] X. P. Zhang and L. N. Yuen Wong, "Cracking processes in rock-like material containing a single flaw under uniaxial compression: a numerical study based on parallel bonded-particle model approach," *Rock Mech Rock Eng*, vol. 45, pp. 711–737, 2012.

[178] M. R. Vergara, M. Van Sint Jan, and L. Lorig, "Numerical model for the study of the strength and failure modes of rock containing non-persistent joints," *Rock Mechanics and Rock Engineering*, vol. 49, no. 4, pp. 1211–1226, 2015.

[179] C. Jin, S. Li, and J. Liu, "Anisotropic mechanical behaviors of columnar jointed basalt under compression," *Bulletin of Engineering Geology and the Environment*, vol. 77, pp. 317–330, 2016.

[180] A. Munjiza, *The Combined Finite-Discrete Element Method*, Wiley, Chichester, UK, 2004.

[181] D. Elmo and D. Stead, "An integrated numerical modelling-discrete fracture network approach applied to the characterisation of rock mass strength of naturally fractured pillars," *Rock Mechanics and Rock Engineering*, vol. 43, pp. 3–19, 2009.

[182] A. Lisjak, B. S. A. Tatone, G. Grasselli, and T. Vietor, "Numerical modelling of the anisotropic mechanical behaviour of opalinus clay at the laboratory-scale using FEM/DEM," *Rock Mechanics and Rock Engineering*, vol. 47, no. 1, pp. 187–206, 2012.

[183] O. K. Mahabadi, B. E. Cottrell, and G. Grasselli, "An example of realistic modelling of rock dynamics problems: FEM/DEM simulation of dynamic Brazilian test on barre granite," *Rock Mechanics and Rock Engineering*, vol. 43, pp. 707–716, 2010.

[184] A. Karami and D. Stead, "Asperity degradation and damage in the direct shear test: a Hybrid FEM/DEM approach," *Rock Mechanics and Rock Engineering*, vol. 41, no. 2, pp. 229–266, 2007.

[185] S. Guo, S. Qi, Y. Zou, and B. Zheng, "Numerical studies on the failure process of heterogeneous brittle rocks or rock-like materials under uniaxial compression," *Materials*, vol. 10, p. 378, 2017.

[186] Y. Li, H. Zhou, W. Zhu, S. Li, and J. Liu, "Numerical study on crack propagation in brittle jointed rock mass influenced by fracture water pressure," *Materials*, vol. 8, pp. 3364–3376, 2015.

[187] H. Lin, W. Xiong, Z. Xiong, and F. Gong, "Three-dimensional effects in a flattened Brazilian disk test," *International Journal of Rock Mechanics and Mining Sciences*, vol. 74, pp. 10–14, 2015.

[188] H. Lin, W. Xiong, and Q. Yan, "Modified formula for the tensile strength as obtained by the flattened Brazilian disk

test," *Rock Mechanics and Rock Engineering*, vol. 49, pp. 1579–1586, 2015.

[189] Y. Wang, X. Zhou, and X. Xu, "Numerical simulation of propagation and coalescence of flaws in rock materials under compressive loads using the extended non-ordinary state-based peridynamics," *Engineering Fracture Mechanics*, vol. 163, pp. 248–273, 2016.

[190] Y. Wang, X. Zhou, Y. Wang, and Y. Shou, "A 3-D conjugated bond-pair-based peridynamic formulation for initiation and propagation of cracks in brittle solids," *International Journal of Solids and Structures*, vol. 134, pp. 89–115, 2018.

[191] Y. Wang, X. Zhou, and M. Kou, "A coupled thermo-mechanical bond-based peridynamics for simulating thermal cracking in rocks," *International Journal of Fracture*, vol. 211, pp. 13–42, 2018.

[192] Y. Wang, X. Zhou, and M. Kou, "Peridynamic investigation on thermal fracturing behavior of ceramic nuclear fuel pellets under power cycles," *Ceramics International*, vol. 44, pp. 11512–11542, 2018.

[193] Y.-T. Wang, X.-P. Zhou, and M.-M. Kou, "Three-dimensional numerical study on the failure characteristics of intermittent fissures under compressive-shear loads," *Acta Geotechnica*, 2018.

[194] Y. Wang, X. Zhou, and M. Kou, "Numerical studies on thermal shock crack branching instability in brittle solids," *Engineering Fracture Mechanics*, vol. 204, pp. 157–184, 2018.

[195] Y. Wang, X. Zhou, and M. Kou, "An improved coupled thermo-mechanic bond-based peridynamic model for cracking behaviors in brittle solids subjected to thermal shocks," *European Journal of Mechanics-A/Solids*, vol. 73, pp. 282–305, 2019.

[196] X. Zhou, Y. Wang, Y. Shou, and M. Kou, "A novel conjugated bond linear elastic model in bond-based peridynamics for fracture problems under dynamic loads," *Engineering Fracture Mechanics*, vol. 188, pp. 151–183, 2018.

[197] C. Yao, Q. H. Jiang, J. F. Shao, and C. B. Zhou, "A discrete approach for modeling damage and failure in anisotropic cohesive brittle materials," *Engineering Fracture Mechanics*, vol. 155, pp. 102–118, 2016.

[198] J. Meng, J. Huang, S. W. Sloan, and D. Sheng, "Discrete modelling jointed rock slopes using mathematical programming methods," *Computers and Geotechnics*, vol. 96, pp. 189–202, 2018.

[199] J. Meng, J. Huang, C. Yao, and D. Sheng, "A discrete numerical method for brittle rocks using mathematical programming," *Acta Geotechnica*, vol. 13, pp. 283–302, 2018.

[200] J. Meng, J. Huang, D. Sheng, and S. W. Sloan, "Granular contact dynamics with elastic bond model," *Acta Geotechnica*, vol. 12, pp. 479–493, 2016.

[201] J. Meng, J. Huang, D. Sheng, and S. W. Sloan, "Quasi-static rheology of granular media using the static DEM," *International Journal of Geomechanics*, vol. 17, 2017.

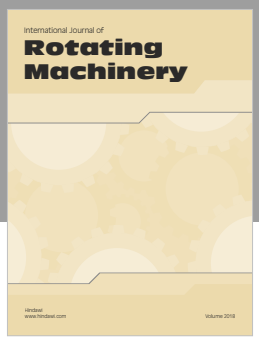

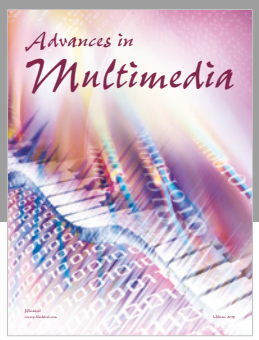

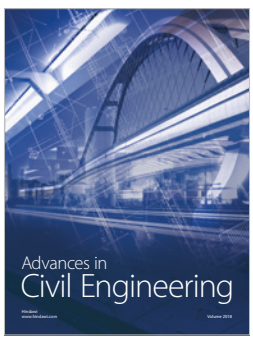

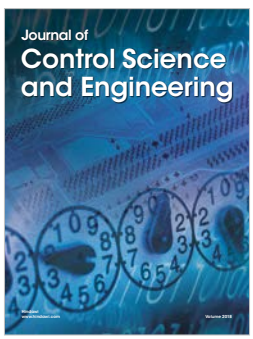

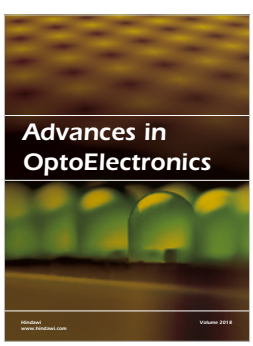

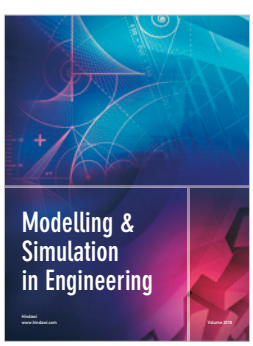

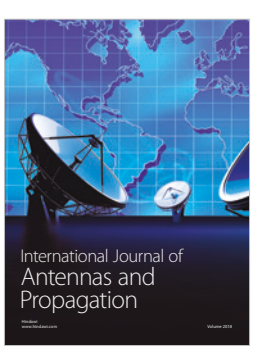

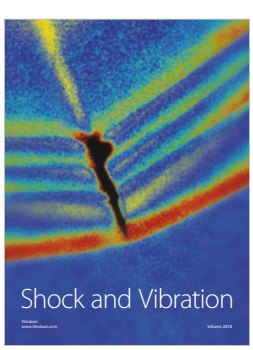

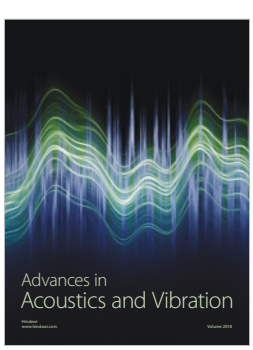

Hindawi

Submit your manuscripts at
www.hindawi.com